Parameter Study of High-ß Tokamak Reactors with Circular and Strongly Elongated Cross Section

H. Herold

IPP 4/153 Mai 1977

MAX-PLANCK-INSTITUT FÜR PLASMAPHYSIK

8046 GARCHING BEI MÜNCHEN

MAX-PLANCK-INSTITUT FÜR PLASMAPHYSIK

GARCHING BEI MÜNCHEN

Parameter Study of High-ß Tokamak Reactors with Circular and Strongly Elongated Cross Section

H. Herold

IPP 4/153 Mai 1977

Die nachstehende Arbeit wurde im Rahmen des Vertrages zwischen dem Max-Planck-Institut für Plasmaphysik und der Europäischen Atomgemeinschaft über die Zusammenarbeit auf dem Gebiete der Plasmaphysik durchgeführt.

IPP 4/153

Parameter study of High-ß Tokamak Reactors with Circular and Strongly Elongated Cross Section

H. Herold

Mai 1977

Abstract

A simplified reactor model is used to study the influence of critical ß values on economy parameters and dimensions of possible long time pulsed tokamak reactors. Various betas deduced from stability and equilibrium MHD theory are introduced and put into the scaling in context with technological constraints, as maximum B-field, core constraint, maximum wall loading a.o. The plasma physical concepts treated comprise circular and strongly elongated cross section and approximated FCT equilibria. The computational results are presented as plots of possible economy parameter ranges (magnet energy, wall loading, volumina, investment costs per unit power) dependent on ß for suitably chosen hierarchies of the constraints. - A burn time reduction by the build ups of α-pressure may be possible for the pressure profile sensitive high-ß equilibria (FCT). Burn times in the 10 sec range, resulting from simple estimates, would about cancel the economic advantages of reactors with high-ß equilibria compared to a ß = 5 % standard reactor (UWMAK I).

C O N T E N T S

1. INTRODUCTION

Parametric studies for tokamak reactors should yield a basis for the optimization of physical and technological reactor parameters, usually with respect to the achievement of minimum costs of power produced. The studies carried through so far (e.g. /1-5/) match one distinct ß-scaling mostly the conventional tokamak scaling ($ß \approx \frac{ß_p}{\sigma^2 A^2}$) with an equilibrium limit of $ß_p$ - with constraints set by technology. Unfortunately the ß-limits and moreover their dependence on plasma profiles, shape and aspect ratio are widely unknown, particularly for the high-ß regime (here defined by $ß_p > 1$, where the plasma is diamagnetic in the toroidal field). So the parameter sets obtained so far may be at least quantitatively misleading. In this study ß is treated primarily as an independent parameter, but various stability and equilibrium betas deduced so far from plasma theory will be discussed for their consequences on reactor economy together with technological constraints, as core constraint, maximum B-field a.o. This procedure gives information on possible parameter ranges dependent on the hierarchy of constraints. Special regard is given to plasma physical concepts which aim at the achievement of high-ß equilibria, namely the strongly elongated plasmas and the FCT-concept.

Although high ß is treated here with respect to magnet field energy utilization, there are other possible advantages of a high-ß regime.

- reduction of absolute reactor dimensions to manageable sizes (transport, repair); saving of rare materials as He, Nb, Pb and others.
- high ß allows operation at the highest possible density and therefore at high collisionality of the plasma. Then favourable aspects with respect to transport are expected:
- reduction of trapped particle phenomena,

- improvement of τ_E in the ohmic heating phase according to experimental results,

- high fractional burn up in a reactor.

According to the wide range and uncertainties in plasma-physics input (e.g. betas from 2 % to 10 % are under discussion which give a P_t-variation of 25) the most simple reactor model is adequate. Here a time independent point model with profile factors from integration and a strongly simplified geometry is chosen. Such a model presupposes that the internal energy balance of the plasma can be maintained with moderate feedback of power to the plasma; i.e. quasistationary burning or longtime pulsed tokamak reactors are treated. For global considerations a duty factor (burn time to cycle time) is put into the scaling.

2. REACTOR MODEL AND CONSTRAINTS

2.1 Reactor model

The reactors are described in a simplified time independent "point model". It is based on the toroidal configurations shown in Fig. 1a for circular cross section (CC), and Fig. 1b for elongated cross section (EC). Rectangular(racetrack) cross section is chosen for the latter because of its improved stability behaviour /6/ compared to elliptic shapes. The definition symbols and units of the model parameters are given as follows (Tab. 1).

The parameters P_t, P_w, B_m, α, D, ε, H, β_p, q_a, f_p (resp. β_o or β instead of β_p and q_a) are chosen as independent parameters and are used as input to the model equations.

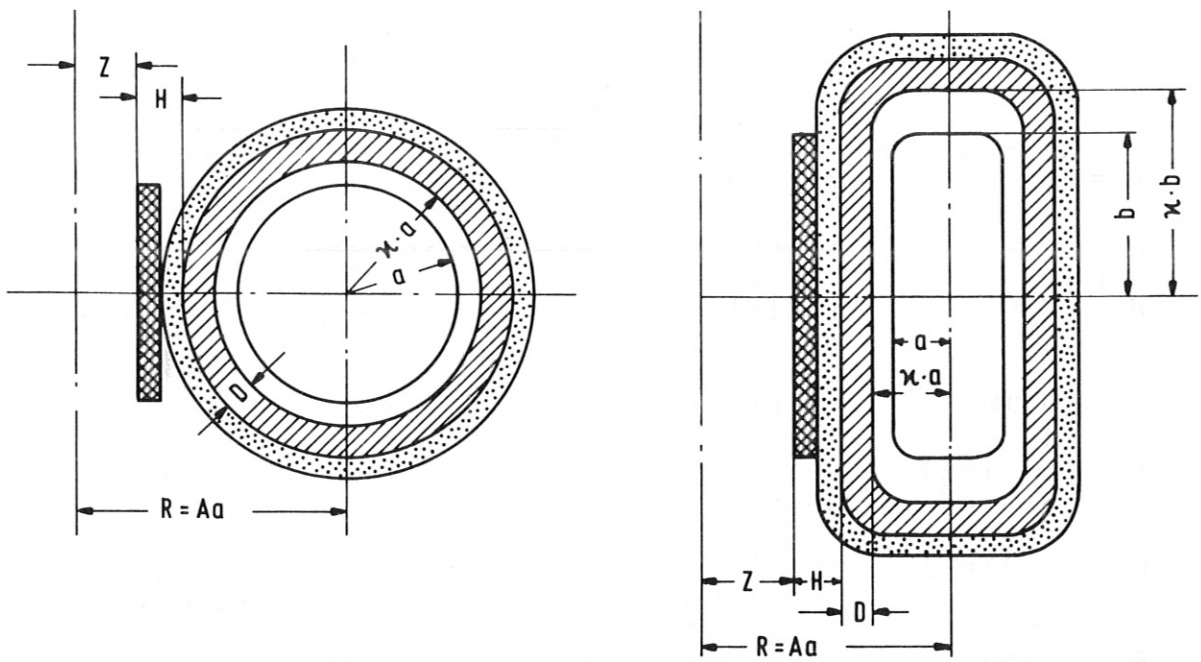

Fig. 1 Tokamak reactor scaling models

a) circular cross section (CC) b) elongated (racetrack) cross section (EC)

Tab. 1 Symbols, units and definitions

$A = R/a$	aspect ratio (R = major torus radius)
a [m]	at CC: plasma radius
a,b [m]	at EC: horizontal resp. vertical semiaxis
$\mathcal{H} = \frac{a_w}{a} = \frac{b_w}{b}$	compression ratio a_w, b_w wall radius; (a_w-a) and (b_w-b) define an outer plasma sheath with no power production (space for divertor sheath limiter, curtains, heating and fueling structure etc.)
$\varepsilon = \frac{b}{a}$	elongation
D [m]	blanket and shield thickness
H [m]	radial thickness of main coil and OH-coil on the inside of the torus
P_t [MW]	thermal power of the reactor
$P_w = \frac{P_t}{O_w}$ $[\frac{MW}{m^2}]$	wall loading; (O_w = surface of first wall) neutron wall loading $P'_w = 0{,}7 \cdot P_w$
Q_T [MeV]	total energy released per fusion reaction including that in the breeding blanket.
B_o [T]	externally applied tor. magnet. field at the geometric center of the torus
B_m [T]	maximum tor. field on the inner surface of the magnet coils
T_i, T_e [keV]	ion, electron temperatures
n $[m^{-3}]$	plasma density
I [MA]	toroidal plasma current
V_p $[m^3]$	plasma volume
f_p	profile factor in equ. (1)
ν, δ, u	exponents in distribution functions for density, temperature and current
$\eta = \frac{\Delta\phi}{\Delta\phi_{ind}}$	total volt sec needed / inductive volt sec.
$\tau = \tau_b/\tau_c$	duty factor; ratio of burn time to cycle time.

Fig. 1a,b

more definitions on Tab. 2

Plasma profiles of the form $n(r) = n_o\ (1-(\frac{r}{a})^2)^\nu$, with $n = n_e = n_i$ and $T(r) = T_i = T_e = \text{const}$ are considered. The assumption of a flat temperature profile is reasonable, when a magnetic limiter or a divertor is applied /7/, but it is not consistent with a peaked resistive current profile. For the thermal power of the reactor we get:

$$P_t = f_p \cdot \frac{n_o}{4}\ \overline{\sigma v}\ Q_T \cdot V_P \qquad (1)$$

$$\text{where } f_p = \frac{2}{a^2}\int_o^a \left(\frac{n(r)}{n_o}\right)^2 r\,dr \text{ is the profile factor.}$$

$T = 15$ keV, $\overline{\sigma v} = 2.66 \cdot 10^{-16}\ cm^3\ sec^{-1}$ and $Q_T = 20$ MeV for D,T ($n_D = n_T = \frac{n}{2}$) are held fixed.

The plasma ß is defined as:

$$ß = \frac{\langle p\rangle}{(B_o^2 + B_p^2)/2\mu_o} \approx \frac{\langle p\rangle}{B_o^2/2\mu_o} \text{ and } ß_o = \frac{p_o}{B_o^2/2\mu_o} \qquad (2)$$

where $\langle p\rangle$ = volume average plasma pressure and p_o and $ß_o$ are local values at the plasma center. $ß/ß_o$ and f_p are given in Fig. 2 as function of ν, consistent with the above profiles.

The poloidal ß and the safety factor are defined as:

$$ß_p = \frac{\langle p\rangle}{B_p^2/2\mu_o}\ ; \qquad (3)$$

$$q_a = \frac{B_a}{B_{P_a}}\ \frac{\ell p}{\ell_t}\ ;\quad q_o = \frac{2B_\varphi}{\mu_o a A}\ \frac{1}{j_o}$$

where ℓ_p and ℓ_t are the poloidal and the toroidal plasma circumference respectively, B_p is the average over a magnetic surface of the poloidal magnetic field and j_o is the current density at the plasma center.

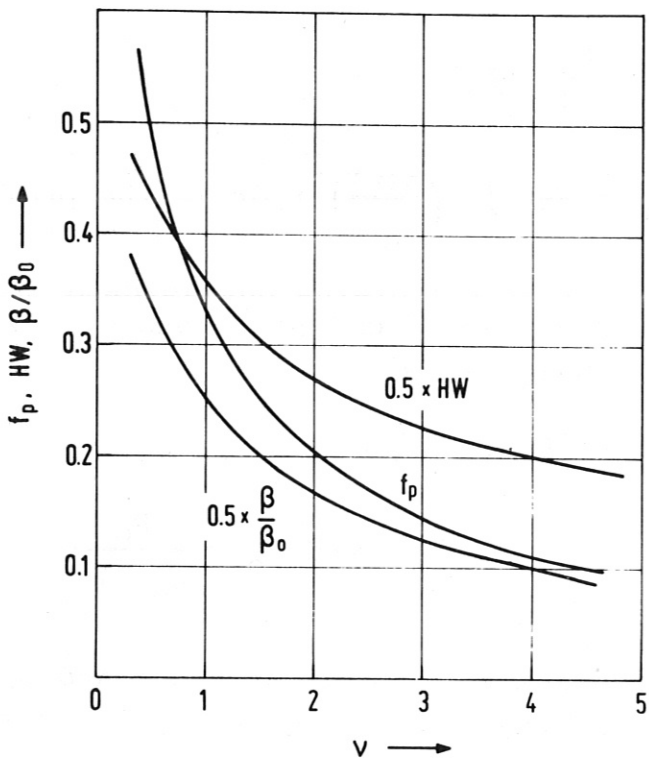

Fig. 2 Profile factor f_p, pressure half width HW, and β/β_o for plasma profiles with $n = n_o(1-(\frac{r}{a})^2)^\nu$, $T = T_e = T_i$ = const., circular cross section.

The plasma current is related to q_a by

$$I = \frac{B \cdot a}{\mu_o q_a A} \cdot f(\varepsilon) \quad \text{where } f(\varepsilon)_{CC} = 1 \text{ and } f(\varepsilon)_{EC} = \frac{4(1+\varepsilon)^2}{\pi^2} \qquad (5)$$

The current density distribution is not specified independently in this study. It is simply assumed that a distribution can be achieved which is consistent with a given q_a/q_o ratio for stability; for instance a current distribution with $j = j_o(1-(\frac{r}{a})^2)^u$ and $q_a/q_o = u + 1$ in the cylindrical approximation.

The ratio q_a/q_o is affected by the structure of toroidal equilibrium magnetic fields particularly by the shift and deformation of the magnetic surfaces in high-ß equilibria. q_a/q_o is to be obtained from numerical equilibrium codes. For low aspect ratios and low ß the ratio $(q_a/q_o)^*$ in plasmas with circular and moderately elongated cross section is approximately given /8/ by:

$$(q_a/q_o)^* = k \frac{4}{\pi} \frac{(A^2+1)^{3/2}}{(A-1)^2(A+1)} \left[1 - \frac{A^{1/2}}{(A+1)}\right] \qquad (6)$$

with $k \approx 1$ for flat current profile
$k \approx 2$ for parabolic profile

The "enhancement" of q_a/q_o compared to the cylindrical approximation is quite strong, e.g. a factor 1.5 at A = 3.

Taking equation (1) - (5) and the geometrical relations consistent with Fig. 1 a set of simplified reactor equations can be obtained which specify the important scaling parameters (Tab. 2).

Lengths in m; powers in MW (*) normalized to power output; (⁻) average over cycle		CC	EC ($\varepsilon = \frac{b}{a}$)
$B_0 = f_1 \left(\frac{P_t}{f_p \cdot \tau}\right)^{1/4} \frac{q_a}{\beta_p^{1/2}} \left(\frac{A}{a}\right)^{3/4}$ [T] (7)	f_1	0.431	$\frac{0.64}{\varepsilon^{1/4}(1+\varepsilon)}$
$B_m = B_0 / (1 - x/A - D/Aa)$ [T] (8)			
$\bar{P}_w = f_2 \frac{P_t}{a^2 A x}$ $\left[\frac{MW}{m^2}\right]$ (9)	f_2	$\frac{1}{4\pi^2}$	$\frac{1}{8\pi(1+\varepsilon)}$
spec. magnetic energy within the toroidal coil $E^* \approx \frac{B_0^2 V_B}{P_t} = f_3 \frac{q_a^2 P_t^{1/2} a^{3/2} A^{5/2} x^2}{\beta_p \tau^{1/2} f_p^{1/2}} \left[\frac{MJ}{MW}\right]$ (10)	f_3	$1.45\left(1+\frac{D}{2xa}\right)^2$	$4.13\left(1+\frac{D}{xa}\right)\left(\varepsilon+\frac{D}{xa}\right)\varepsilon^{\frac{1}{2}}(1+\varepsilon)^2$
spec. blanket volume $V_D^* = \frac{V_D}{P_t} = f_4 \frac{D}{\bar{P}_w}$ $\left[\frac{m^3}{MW}\right]$ (11)	f_4	$\left(1+\frac{D}{2xa}\right)$	$\frac{\left(1+\varepsilon+\frac{D}{xa}\right)}{(1+\varepsilon)}$
"power density" in the plasma $W_p = \frac{P_t}{V_p} = f_5 (\bar{P}_w x)^{3/2} \left(\frac{A}{P_t}\right)^{1/2} \left[\frac{MW}{m^3}\right]$ (12)	f_5	12.57	$\frac{5.0(1+\varepsilon)^{3/2}}{\varepsilon}$
plasma energy ($3nkT \cdot V_p$) $E_p = f_6 \left(\frac{P_t A}{\tau f_p}\right)^{1/2} a^{3/2}$ [MJ] (13)	f_6	$\frac{2.18}{(\nu+1)}$	$2.46\,\varepsilon^{1/2}/f(\nu,\varepsilon)$ $f(\nu,\varepsilon) \approx 1$

Tab. 2 Simplified tokamak reactor equations for circular and elongated cross section

2.2 Constraints

As leading constraints, which may limit the working space available for reactor designs, we take (not in hierarchic order; see 3.1.1 for the hierarchy of constraints):

1) The core constraint

2) Equilibrium and stability requirements for the tokamak
   1) and 2) are treated in 2.21 and 2.22.

3) B_m, the maximum magnetic field on the inside of the toroidal field coils in the range B_m = 6; 8; 12 [T]. B_m depends on the choice of superconducting material. For Nb-T_i superconductor $B_m \leq 8$ T is assumed /9/. Here mainly B_m = 8 T is considered because generally $F^* = \frac{E}{P_t} \sim \frac{1}{B_m^2}$.

4) P_w, the average wall loading. A maximum allowable P_w may be given by the admissible integral wall loading $P_w \cdot t$ for a reasonable lifetime of the first wall, i.e. not too short exchange times /10/. Values of $P_w \cdot t$ by 2,5 to 10 $[\frac{MWa}{m^2}]$ and minimum exchange times of 1 to 2 years are under discussion /10/, /11/. That would lead to a range of maximum P_w of 1.25 to 10 $[\frac{MW}{m^2}]$. On the other hand for economic reasons, as compactness of the reactor and minimum investment costs (spec. blanket costs: $K_D \sim V_D^* \sim \frac{D}{P_w}$), P_w should be chosen as high as possible.

   The influence of P_w and associated wall exchange on the running costs of a power station /10/ is not considered. It is supposed here that a reasonable design strategy would take maximum advantage of the reduction of investment costs (by high P_w) and separately try to minimize the exchange costs by appropriate measures (curtains, spectral shifter, minimum thickness of structures to be exchanged).

Further conditions and parameters are treated as standard. They are normally held fixed. The range of eventual variations is given in parentheses:

- Plasma temperature: $T = T_i = T_e = 15$ keV. This is about the optimum temperature for a pressure limited reactor plasma. $Q_T = 20$ MeV. Profile factor $f_p = 0{,}5$ (0,1 ÷ 1 see 3.1.3). In UWMAK I the same f_p is used. $f_p = 0{,}5$ is used for elongated cross sections too, which is possibly an underestimate.

- Thermal reactor power $P_t = 5$ GW $(1 < P_t[GW] < 10)$

- Blanket and shield thickness $D = 1.5$ m $(1 < D[m] < 2.5)$

- Compression ratio $\varkappa = 1.2$ (1.1 to 1.5)

- Thickness of toroidal coils and OH coils on the inside $H = 1.5$ m /2/ (no variation, because design aspects (dewar) rather than stress may determine the space needed).

- Burn time to cycle time ratio $\tau \approx 1$ which corresponds to a long time pulsed reactor. The impact of shorter burn times is studied for FCT equilibria.

- The reactor format is given in Fig. 1a and b. For elongated cross section a racetrack (rectangular) shape is chosen $\varepsilon = 4$ ($\varepsilon = 2$ to 6)
  Elongation between 1 and 2 is considered to be equivalent to circular cross section for the purpose and within the accuracy of this study.

With the above reactor model some "economy parameters" can be deduced. They presumably determine the major investment costs of the reactor core. They may serve for a rough comparison of different reactor designs. The investment costs can be related by means of these parameters to those of a standard design, with parameters close to UWMAK I /4/. One important economy parameter is: E^*, the specific magnet

energy of the main field stored within the plasma and the blanket, which is the absolute minimum of magnetic energy needed. In a realistic toroidal reactor the stored energy is certainly higher because space is needed for reasons of coil shape, accessibility, heating and fuelling equipment, divertors etc. For the purpose of comparison the use of E^* precludes that this additional volume is proportional to E^*.

Another important parameter is the specific blanket volume V_D^* or the inverse fusion power density in the blanket, which is related to P_w like

$$V_D^* \approx \frac{D}{P_w} f(a, \mathcal{L}, \varepsilon) \quad \text{where } f \approx 1. \quad \text{see (11) tab. 2.}$$

Other parameters, which can be deduced, are the plasma energy Ep (equ. 13, tab. 2) to be maintained by heating, refueling and α-energy deposition; and the plasma current I (equ. 5), which determines the size and the design of the ohmic heating transformer and the amount of stored poloidal magnet energy.

2.2.1 Core constraint

The tokamak plasma forms the single turn secondary of the OH-transformer. The requirement in flux change (volt-seconds) to induce the toroidal current is approximately given by

$$\Delta\phi = \Delta\phi_{ind} + \Delta\phi_{r,1} + \Delta\phi_{r,2} \approx I \cdot L + \int_0^{\tau_h} I(t) \cdot R(t)\, dt + \int_{\tau_h}^{\tau_b} I \cdot R\, dt \qquad (14)$$

L is the plasma inductance, τ_h heating time, τ_b burn time, R total plasma resistance. The second and the last term of (14) are the resistive volt-second requirements. The inductive flux change, $\Delta\phi_{ind} = I \cdot L$, is a rough approximation, which is sufficient here. A more exact treatment regarding the reduction of $\Delta\phi$ by the mutual coupling of primary and secondary is given in /12/ and /13/.

$\Delta\phi_r$ depends on the time behaviour of the plasma. For the present study only the rough limits in terms of $\Delta\phi_{ind}$ shall be assessed:

During plasma burn with constant and homogeneous plasma parameters we get:

$$\Delta\phi_{r,2} \approx I \cdot \rho_{\parallel} \cdot \delta \cdot \frac{\pi A}{2\varepsilon a} \cdot \tau_b \quad \text{with} \quad \rho_{\parallel} = 1.05\ 10^{-8}\ T_e^{-3/2} \ [\Omega m] \ (T_e \text{ in eV})$$

and L given as $L \approx 0{,}2\pi\ A^2 a/\varepsilon$[Hy]

$$\frac{\Delta\phi_{r,2}}{\Delta\phi_{ind}} \approx \frac{10^{-2}\,\delta\tau_b}{2\pi A a^2} \quad \text{for } T_e \approx 15 \text{ keV, a[m]; } \tau_b \text{ [sec]}$$

δ is the anomaly factor of resistance (usually assumed to be about 5, if the effect of a low impurity content is included). With reactor dimensions (A = 3; a = 5 m) we get:

$\Delta\phi_{r,2} \Big/ \Delta\phi_{ind} \approx 10^{-4}\ \tau_b$. Thus $\Delta\phi_{r,2}$ may be disregarded for $\tau_b < 1000$ sec.

$\Delta\phi_{r,1}$ for the current rise is more difficult to assess. In the present experiments $\frac{\Delta\phi_{r1}}{\Delta\phi_{ind}} \approx 0{,}5$. For a reactor 1/5 of the thermal plasma energy may be supplied by a linearly rising heating current. An effective resistance

$$R_{eff} = \frac{3}{5}\,\frac{Ep}{I^2 \cdot \tau_h} \quad \text{and} \quad \Delta\phi_{r,1} = \int_0^{\tau_h} I(t)\ R_{eff}\, dt \approx \frac{3}{5}\,\frac{Ep}{I}$$

$$\text{and} \quad \left(\frac{\Delta\phi_{r,1}}{\Delta\phi_{ind}}\right)_{CC} \approx \frac{Ep \cdot 10^6}{A^2 a I^2} \approx 0{,}4\ \beta_p \quad \text{(circular cross section)}$$

$$\left(\frac{\Delta\phi_{r,1}}{\Delta\phi_{ind}}\right)_{EC} \approx \frac{0{,}5\varepsilon Ep \cdot 10^6}{A^2 a I^2} \quad \text{(for elongated cross section)}$$

With Ep[Joule]; I[A]; a[m], can be deduced.

Thus for reactor dimensions $\Delta\phi_r / \Delta\phi_{ind} \approx 0{,}5 - 0{,}8$ for both cross sections.

So $\Delta\phi$ may be expressed by

$$\Delta\phi = \eta \cdot \Delta\phi_{ind} = \eta I \cdot L \quad \text{where } \eta = 1.5 \div 1.8 \tag{15}$$

The plasma inductances for the circular and elongated cross section with homogeneous current distribution are approximately:

$$L_c = 4\pi \cdot 10^{-7} \, Aa \, (\ell n \, 8A - 1.75) \quad [Hy] \tag{16}$$

$$L_E = 1.25 \cdot 10^{-6} \, \frac{a \, A^{7/4}}{(1+\varepsilon)^{3/4}} \quad [Hy] \tag{17}$$

So the minimum necessary core radius Z (see Fig. 1a,b) may be expressed by:

$$Z \geq Z_o = \left(\frac{\eta \, \Delta \phi_{ind}}{\pi \, \Delta B}\right) \quad \text{and} \tag{18}$$

$$Z = R - (\varkappa a + D + H) \tag{19}$$

For the flux density swing the following assumptions were made:

a) Air core and bidirectional flux density swing $\Delta B = 16$ [T]which would be appropriate for superconducting OH-coils ($\hat{=} \, 2 \, B_m$ for NbTi superconductor)

b) Iron core with reverse saturations prior to charging, ΔB limited by the saturation level of iron: $\Delta B = 3{,}2$ [T];

Usually in the following parametric studies the core constraint is calculated for $Z = Z_o$, using (16), (18), (19), (17) and (5) with $q_a/q_o = 3$ and $\eta = 2$, if not otherwise specified.

2.2.2 Equilibrium and Stability

For reasonable dimensional scaling of Tokamak reactors information is needed on the upper limits of ß for arbitrary aspect ratio, shape of the cross section and pressure profile, since these quantities enter the expression for the power output of a reactor. The present status of MHD stability and equilibrium theory is by far not sufficient to make generally valid scaling considerations. Most probably an economic reactor should work in the regime of high-ß--equilibria ($ß_p > 1$). Particularly for this regime only limited knowledge from theory (mostly in numerical examples only and practically no experimental experience is available.

Without going into the physics some features from MHD-theory (particularly for gross ideal MHD stability, but no axissymmetric modes) important for the reactor are listed as follows:

2.2.2.1 Standard low ß equilibria

Most of the scaling and optimization studies e.g. /1/, /2/, /3/ also for reactor designs /4/ are done with the "conventional tokamak scaling". This takes results of low ß, high aspect ratio (cylindrical) ideal MHD stability theory for standard equilibria /16/. $q_a/q_o \geq 2{,}5$ is required for stability against external kink modes (peaked current profile see 2.1) and $q_o \geq 1$ for stability against internal modes (Tokamak experiments are mostly carried through at q_a values of 4 to 6 where the lower limiting values are usually set by strong disruptions). Limiting $ß_p$ are taken from equilibrium theory /4/ which shows that the occurrence of current reversal on the inside of the torus limits $ß_p$ to:

$$ß_p \leq A/2 \tag{20}$$

From (2), (3) and (4) the ß values in the mostly used conventional scaling are given by:

$$ß_{c,1} = \frac{1}{2q_a^2 A} \left(f(\varepsilon)\right)^2 \text{ where } f(\varepsilon) = \frac{\ell_p}{2\pi a} \tag{21}$$

In (21) it is assumed that the minimum achievable q_a does not depend on the elongation. This assumption is supported by experimental findings /6/, /15/.

Another β_c-scaling often used /5/ is derived from the neoclassical kink mode stability limit, where for $\beta_p \sim \sqrt{A}$ the bootstrap current will cause the onset of kink modes /14/. It is given by:

$$\beta_{c,2} = \frac{\sqrt{2}}{A^{3/2}\, q_a^2} \qquad (22)$$

Toroidal MHD-stability of axisymmetric low-ß-equilibria was analysed by Wesson /16/ by means of a numerical code. Since toroidal effects cause a larger q_a for a given current distribution than for a cylinder (see 2.1), unstable kink modes may be limited to a higher m-value. Furthermore for small aspect ratio the tearing modes should be stable for $q_o \geq 1$ ($q_o \geq 3$ is needed for large A to avoid m-2 or m-3 tearing modes, which is usually not regarded when using $\beta_{c,1}$). Wesson proposes:

$$\beta_{c,3} = 0.21/A^2 \qquad (23)$$

2.2.2.2 High-ß-equilibria and their MHD stability

In high-ß equilibria ($\beta_p > 1$) the plasma is diamagnetic in the toroidal field. The plasma pressure is mainly supported by the toroidal field (note, that the usual assumption $\beta_p \leq A$ (no second magnetic axis) already precludes low ß equilibria). Qualitative features of high-ß equilibria are (progressively more pronounced with increasing plasma pressure) /17/:

- the flux surfaces are deformed from circular towards elongated shapes which are shifted outward,

- the plasma current increases in the outer region of the torus, and the current peak separates from the peak of the pressure distribution,

- reverse currents may appear on the inside of the torus,

- $\beta_p = \frac{2\mu_o \langle p \rangle}{B_p^2}$ may not be limited by equilibrium consideration.

$\beta_p > A$ have been demonstrated /17/, /6/.

Numerically computed equilibria /18/ indicate that there is an inverse relation between the width of the current and pressure profiles. Reasonable, not too skinned current profiles, are reached for a pressure profile half width, HW, normalized to the plasma radius of about HW = 0.5, which according to (1) and Fig. 2 gives strongly reduced power outputs. Examples for current and pressure profile /2.18/ are shown in Fig. 3.

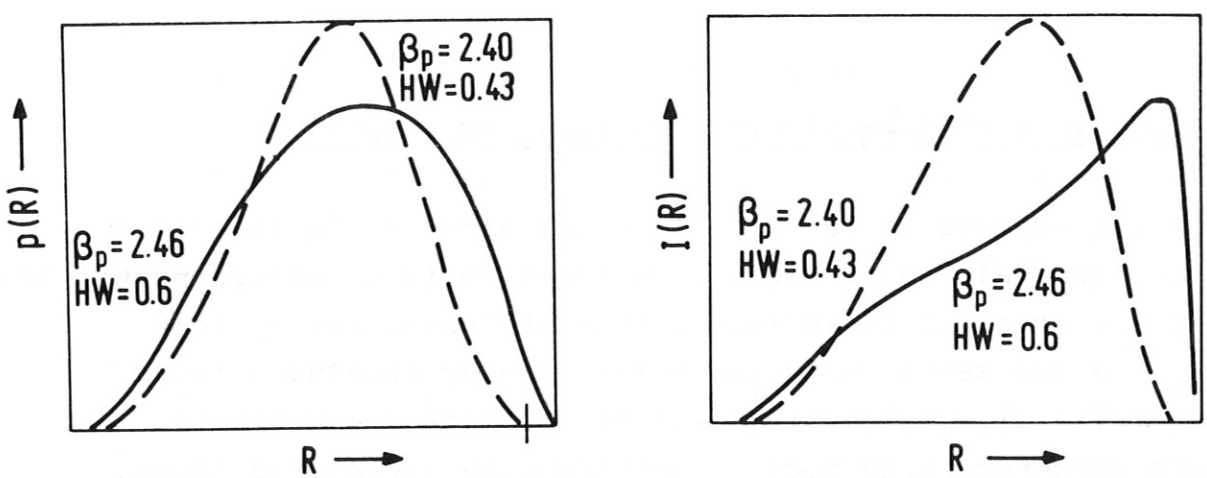

Fig. 3 Pressure and current profiles in D-shaped high-ß equilibria with A = 3, /18/.

In /19/, /20/ it is shown that high-ß-equilibria are possible for highly elongated cross sections, even at high compression ratios (e.g. $\varepsilon = 4, \mathfrak{N} = 3$). For a plasma surrounded by a force free field with constant pitch much higher elongations can be achieved /20/.

Flux conserving equilibria /21/, /22/ are obtained when the transition from low ß to high ß equilibrium is done by rapid heating. Then, not only the magnetic flux linking a plasma pressure surface, but also the initial q-profile will be preserved. When the pressure increases, additional current is induced on the outside of the plasma torus by the structural changes of the configuration itself. This current must be balanced by an equal opposite current flowing in external windings. The total current in a FCT must increase roughly $\sim$ (plasma pressure)$^{1/3}$ /23/. The structure of the cross section changes progressively as outlined before, but reverse currents on the inside of the torus do not appear. To achieve high ß (> 5 %) the half width of the pressure profile must lie between 0,4 and 0,55 /22/.

Presumably the FCT equilibria are not compatible with long time finite resistivity equilibrium /7/. The time scale in which the flux configuration changes sufficiently to modify the equilibrium distribution of magnetic fields (configuration time) may be approximated by

$$\tau_c \approx \frac{40\ Te^{3/2} \cdot s^2}{Z \cdot \delta} \quad [\text{sec}]$$

δ anomaly factor with regard to Spitzer resistivity
Z effective charge state
s characteristic length in m
T_e in keV

If for s the difference of the admissible half widths s = (0,55 - 0,4) a = 0,15 a is taken, and for $Z \cdot \delta \approx 5$, configuration times of 100 to 500 sec should be achievable under reactor conditions.

Whether the configuration can be maintained by control measures for longer times is questionable; MHD stability results for FCT-high-ß-equilibria did not appear so far. It is likely that the configuration is susceptible to kink-balooning instabilities.

MDH stability analyses relevant to high-ß equilibria (high-ß ordering: $ß = \frac{1}{A}$ see /24/) were carried through in approaches of different sophistication:

1) Sharp boundary, skin current model for a class of toroidal, axisymetric high-ß equilibria (not FCT) with arbitrary cross section, constant pressure, plasma surrounded by vacuum /24/, /25/.

   An upper limit of ß exists for stability against gross kink modes. Internal modes are not treated. For circular cross sections:

$$ß_{c,4} \approx \frac{0.21\ n^2}{A} \qquad (24)$$

   n is the toroidal mode number.

   Elongated cross sections help to improve the stability. For the ellipse there is an optimum elongation $\varepsilon = 2.2$ for which $ß_c$ has a flat maximum and

$$ß_{c,4'} \approx \frac{0.37\ n^2}{A} \qquad (25)$$

   In both cases $ß_c$ is nearly independent of q_a (for (24) beyond $q_a = 1.7$). The optimum elongation is higher for the doublet configuration ($\varepsilon = 4$) and presumably for racetrack cross sections too, because their radius of curvature is more favourable than that of the elliptic cross section. Triangularity deteriorates gross MHD stability. Conducting walls have a weak influence.

   Peliminary results with force free fields instead of vacuum outside /26/ point towards further improvement of $ß_c$.

Thin skin stability results are generally thought to be too optimistic /26/ regarding quantitative statements (e.g. ß-limit). But some of the mentioned tendencies may be valid.

2) Diffuse current model for a class of toroidal, axissymmetric high-ß equilibria (not FCT), circular cross sections, infinite conductivity, plasma surrounded by vacuum /24/. Included are global kink balooning modes (no internal modes, no axissymmetric n ≠ o modes). Parameter space is $ß \cdot A$; q_o; a_{eff} (pressure weighed current profile width) and r_w/a (wall/plasma radius). Observing $q_o \geq 1$ and current reversal:

$$ß_{c,5} \cdot A \approx 0{,}1; \quad \text{and } q_a > 3 \quad \text{is proposed/28/} \qquad (26)$$

Wall proximity is stabilizing (for instance $r_w/_a = 1.2$ for (26)). If higher m-modes are taken seriously steep pressure profiles (HW ≈ 0,5) and steeply increasing q-profiles ($q_a > 3$, for shear) are necessary. Flat current distribution cannot be stabilized without a close conducting wall ($r_w/_a \approx 1$).

Numerical stability analyses with 3-dimensional codes which are in progress should give more insight in the gross MHD stability behaviour of high-ß equilibria in the near future.

Stability analyses for localized interchanges (test against violation of the Mercier criterion) have been done for numerically obtained high-ß equilibria with diffuse profiles which fulfill $q_o = 1$, /18/29/. The highest $ß_c$ were found for the flattest pressure profiles compatible with equilibrium. $ß_c$ improves in D-shaped plasmas (dip outward) with triangularity (contrary to skin current gross MHD--stability) and with a limited elongation. In /18/ the peak

$\beta \approx 12$ % is reached for a D-shaped plasma with $\varepsilon = 1.65$ ($\beta_p = 2.4$; $A = 3$). The peak β_c for Doublet is 4.7 % ($A = 3$; $\varepsilon = 3$, $\beta_p = 1$).

SUMMARY

The results of equilibrium and MHD stability theory (for global stability) most important for the present reactor scaling are summarized as follows:

- Present stability analyses predict that limiting betas exist, below which gross ideal MHD stability should be possible, but for stabilization of kinks in high-ß-equilibria a judicious choice of q_a, wall position and high ß has to be made. $q_o \gtrsim 1$ for stability of internal modes seems to be necessary whatsoever cross section, shape and pressure profile. Flat current profiles are destabilizing for gross modes in ideal MHD, but the internal resonant surfaces in peaked profiles may cause negative effects (e.g. disruptions, tearing modes). So the question for "optimum profiles" is open. The favourable influence (cf. $\beta_c \sim \frac{1}{q^2 A^2}$) of small aspect ratios appears to be reduced at high-ß equilibria, possibly by balooning instabilities.

- All stability analyses indicate that improvements in ß should be possible by elongation and by D-shape. But the optimum ß may be achieved at rather low elongations - at $\varepsilon \approx 2$ for elliptic cross section and at $\varepsilon \approx 4$ for doublet and possibly for racetrack cross section.

- Because resistive modes and their nonlinear growth are not covered for high-ß-equilibria the picture is incomplete and too optimistic. On the other hand finite larmor radius and viscosity may have a beneficial effect on instability growth.

- Plasma betas obtained from equilibrium analyses appear no longer to be limiting. $\beta_p > A$ have been demonstrated theoretically and experimentally, as well as a physically sensible method to produce them (FCT).

3. RESULTS

3.1 Tokamak reactors with circular cross section

3.1.1 Working space and hierarchy of constraints

Fig. 4 and 5 give an instructive overview on the working range for 5 GW tokamak reactors with circular cross section, determined by the constraints (e.g. critical β, B_m and the core constraint). The representation with the central beta, β_o , and P_w as coordinates and the Iso-magnet-energy curves, $E^* = \text{const}$, allows crude optimization within the parameter space given by the constraints. P_w should be maximized to achieve the lowest volumina, and E^* is to be minimized. This representation is used too for elongated cross section, Fig. 8, and FCT equilibria, Fig. 16, because it allows to study the impact of various plasma betas on economic features of the reactor. (Note: β_o is chosen for the plots instead of β, so the profile factor f_p can be varied independently. See Fig. 2 for $\beta/\beta_o = f(f_p)$).

In Fig. 4 the maximum magnetic field, B_m, is taken as parameter for a fixed aspect ratio, A = 3. As an example conventional tokamak scaling, $\beta_{c,1}$ with $\beta_p = A/2$, is implemented by the q_a-ordinate. The limit $q_a = 3$ ($\beta_c \approx 2$ %) is indicated. If there is a critical beta (determined in the plot by q_a) which cannot be surpassed, there are two working points with optimum parameters E^* and P_w (resp. V_D^* or a) given by the intersection of $\beta_o(\beta_c) = \text{const}$ with the core constraint (curve C_s) or with a $B_m = \text{const}$ curve. If $B_m = 8$ T is a leading constraint besides β_c, there is no further limitation by C_s for the whole range of possible betas, but P_w remains low for reasonable $q_a \geq 3$ (large reactor

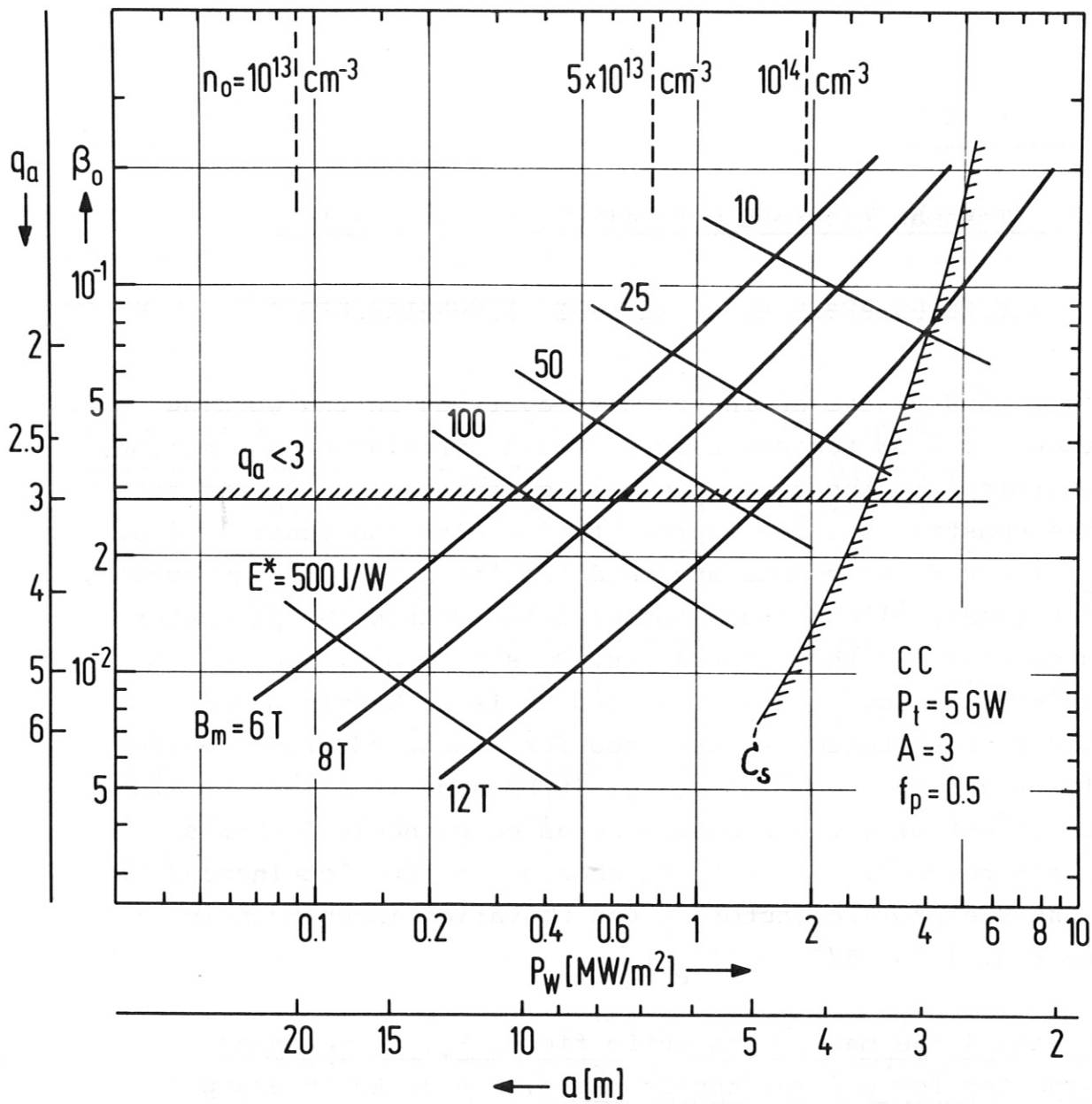

Fig. 4 Working range for 5 GW(th) tokamak fusion reactors with circular cross section, A = 3, f_p = 0.5; β_o is related to q_a for $\beta_p = \frac{A}{2}$, ($\beta = \frac{1}{2q^2A}$). The core constraint C_s is plotted for bidirectional flux density swing: ΔB = 16 T; η = 2; q_a/q_o = 3. $E^* = \frac{E}{P_t}$ = spec. toroidal magnet energy. The hatching points toward the working space excluded by the constraints (e.g. to the right of C_s).

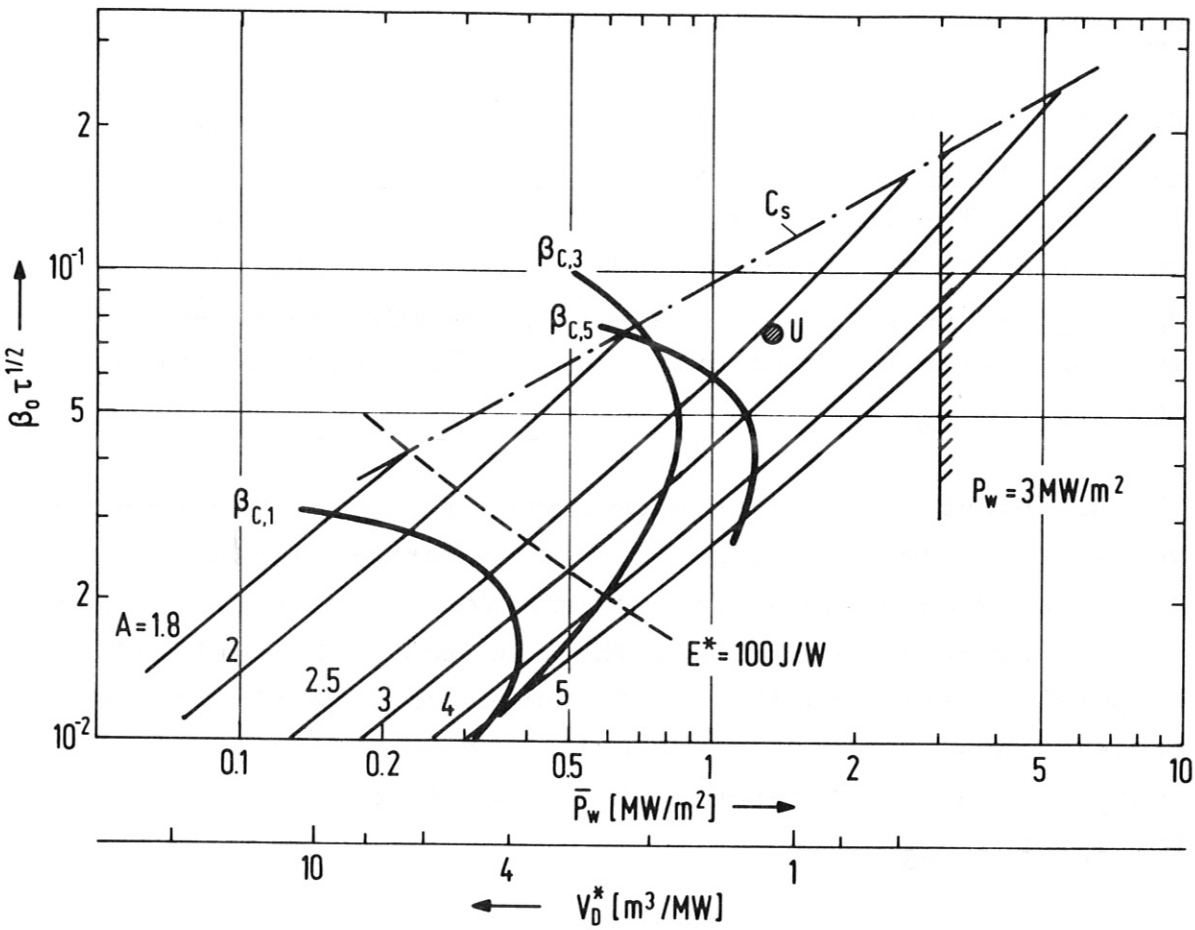

Fig. 5a Working range for 5 GW(th) tokamak reactors with circular cross section B_m = 8 T; f_p = 0.5; A = aspect ratio; C_s = core constraint with ΔB = 16 T; η = 2; q_a/q_o = 3. U position of the standard UWMAK I reactor in the diagram.

$\beta_{c,1} \sim 1/A$ conventional β_c with β_p = A/3;
$\beta_{c,3} \sim 1/A^2$ Wesson's proposal;
$\beta_{c,5} \sim 1/A$ diffuse current model, Freidberg
(see 2.2.2, for explanation of the critical betas)

dimensions). This statement is true for the whole range of thermal powers ($1 < P_t$ [GW] < 10). Going to the limits posed by the core constraint for air core and superconducting (NbTi) OH-coils extremely high magnetic fields, B_m, are needed.

Fig. 5a has the same coordinates as Fig. 4 but now B_m is held fixed at the reasonable $B_m = 8T$ and the aspect ratio is varied. The core constraint (curve C_s) for a peaked current profile (corresponding to $q_a/q_o = 3$) and various $\beta_c = \beta_c(A)$ are plotted. C_s and the most optimistic and the most pessimistic β_c cut out a range of parameters available for limited B_m.

The different β_c-scalings show common features. The lowest volumina (highest P_w) are achieved at rather high aspect ratios between 3 and 4. The minimum for the magnetic energy lies at lower aspect ratios. This can easily be verified by parallel-shifting the iso-E* curve. In an optimization process these two features should be combined to get for instance the lowest investment costs. (This is done below for $\beta_{c,1}$ and $\beta_{c,3}$).

Furthermore, Fig. 5a shows that even the most favourable stability assumptions lead to optimum β_c-values of 3 to 4 % (β_o of 5 to 6 %). The $\beta_{c,5}$ in Fig. 5a, deduced from diffuse, high-β stability theory, is assumed to scale with 1/A like the critical β of the sharp boundary model, $\beta_{c,4}$, which is not included in the plot.

Hierarchy of constraints.

If a search is made for optimum economic reactor parameters clearly a hierarchy of constraints has to be observed. This is illustrated by Fig. 5c which is a simplified version of 5a. Usually optimum parameters are given by the intersection of two constraints, marked by Y, B or P in Fig. 5c. This points characterize what we call B-scaling, Y-scaling etc. For instance Y-scaling means that C_s and β_c

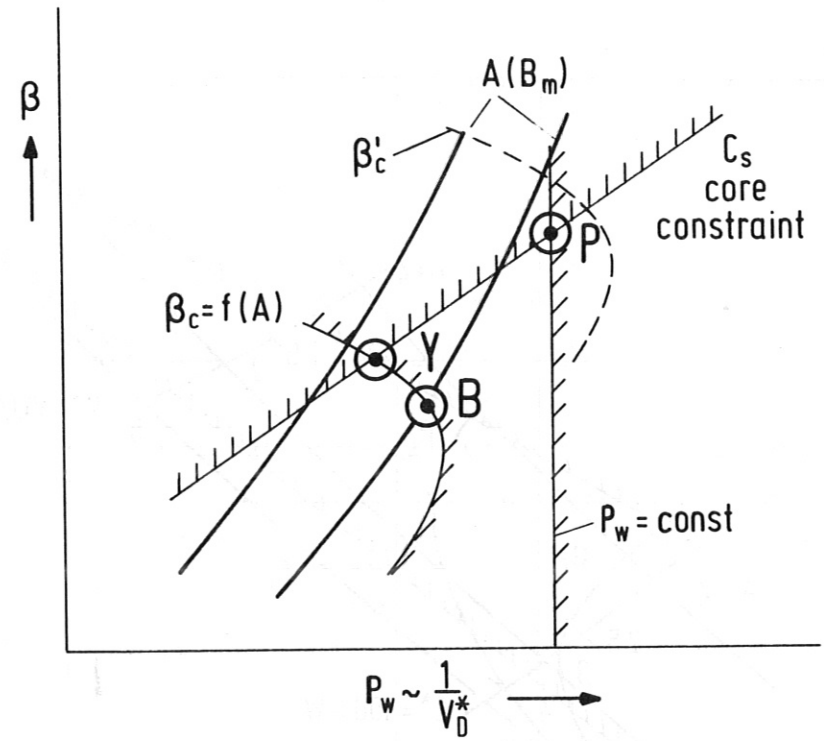

Fig. 5c Hierarchy of constraints and classification of scalings

are considered as leading constraints. Then the working point Y selects correlated reactor parameters ß, A, P_w etc. Additional variations, for instance taking another P_t or B_m, can then be made under the constraints of the chosen scaling.

B-scaling has the leading constraints $ß_c$ and $B_m(A)$. Clearly, for our example, which is valid for the circular cross section, B-scaling yields the optimum parameters. Y-scaling would select lower P_w and possibly lower E^*. It would not be meaningful because economically better parameter sets are admissible. This is no longer true for elongated cross section (cf. Fig.8). Occasionally in parameter studies, which have appeared so far, Y-scaling is used throughout for all cross sections.

P-scaling is appropriate only when the plasma physics allows very high ß (e.g. curve $ß'_c$ in Fig. 5c), so that P_w together with C_s become limiting constraints.

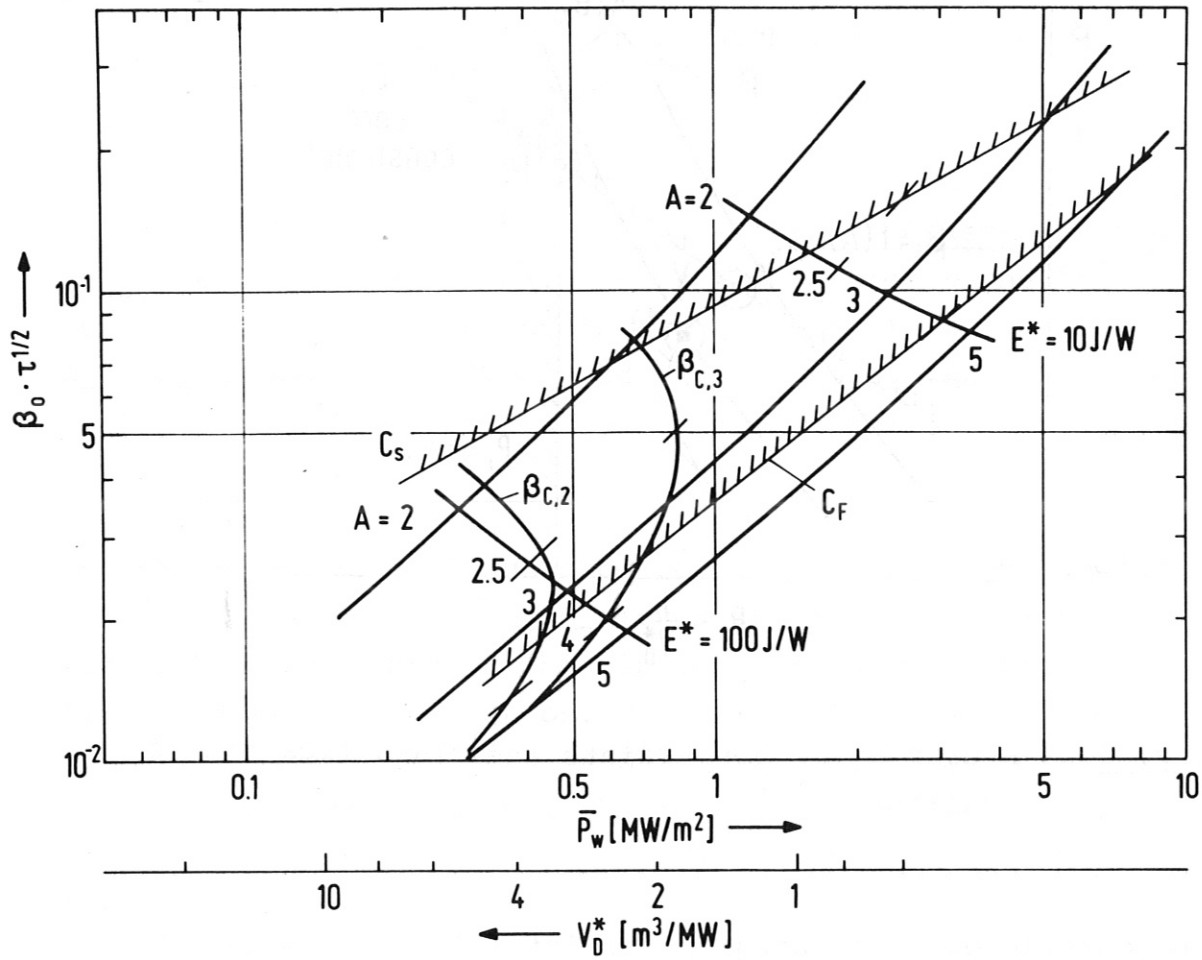

Fig. 5b Working range of 5 GW(th) Tokamak reactors as in Fig. 5a, but with C_F = core constraint for an iron core (ΔB = 3,2 T; η = 2; q_a/q_o = 3); $\beta_{c,2}$ neoclassical kink mode limit, see 2.2.2.

For an iron core the core constraint surely becomes a leading constraint, which would limit the economic features of a tokamak reactor (see Fig. 5b, curve C_F). Now higher aspect ratios and correspondingly lower ß, higher E^*, higher volumina etc. are obtained.

3.1.2 Parameter range and optimization of the aspect ratio for circular cross section

As an illustrative example for B-scaling of various parameters, limiting $ß_c$ have been selected: the optimistic $ß_{c,3}$ typical for $ß_c \sim \frac{1}{A^2}$ and the most conservative: $ß_{c,1} \sim \frac{1}{A}$ with $q_a = 3$ and $ß_p = A/3$. So approximately the whole range which shall be possible is covered as well as the range in A-dependence.

Fig. 6 shows the range of various parameters dependent on A for the two $ß_c$ at $B_m = 8$ [T] and for 5 GW reactors. The conservative parameters for $ß_{c,1}$ are clearly prohibitive.

A rough estimate of the main investment costs for the reactor can be made. If the specific magnet costs K_B are taken to be $K_B \sim E^*$ and the spec. blanket and shield costs $K_D \sim V_D^*$ (V_D^* specific blanket and shield volume), the costs can be related to those of a standard reactor with parameters close to UWMAK I (see table 4). A cost ratio $K_D/K_B = 0{,}6$ like that of UWMAK I is assumed for the standard reactor at A = 2.6. The results for $ß_{c,1}$ and $ß_{c,3}$ and 5 GW reactors are shown in Fig. 7. Obviously there is a big range of about a factor 4, at optimum A, for the most important investment costs. The cost variation with A is caused mainly by K_B. The magnet costs increase roughly a factor ten when going from A=2 to A=5. The blanket costs are insensitive to A-variation in the range A = 2.5 to 5. Whether this feature can be used to conceive reactors with larger A, without having a costs penalty, needs more detailed studies. This would be possible if the additional magnet volume outside the blanket could be reduced for a more slender torus.

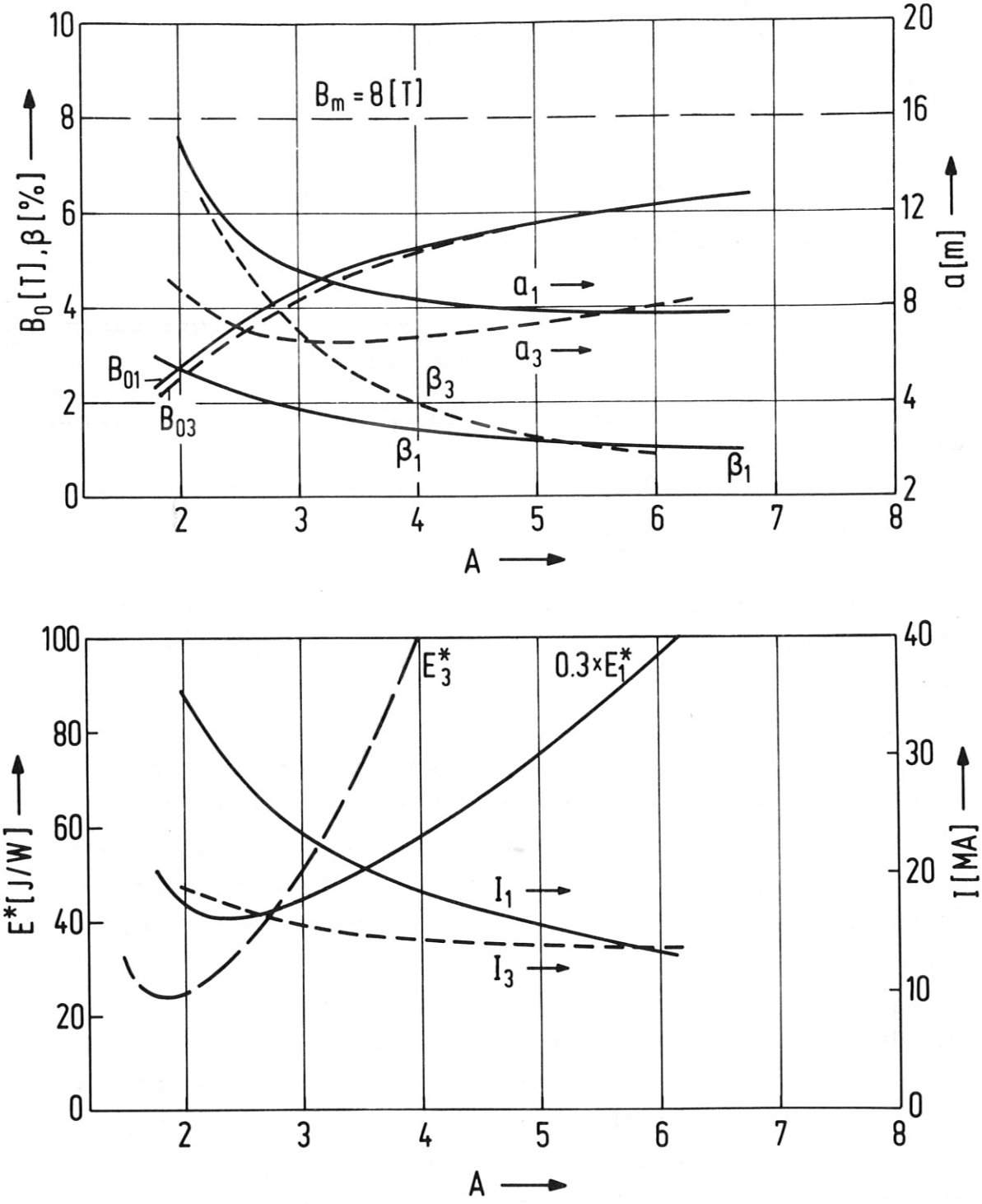

Fig. 6 Reactor parameters as function of A for:
$\beta_{c,1}$ (index 1; $q_a = 3$; $\beta_p = A/3$) and
$\beta_{c,3} \sim 1/A^2$ (index 3)
$B_m = 8$ T; $P_t = 5$ GW; $f_p = 0.5$; circular cross section.

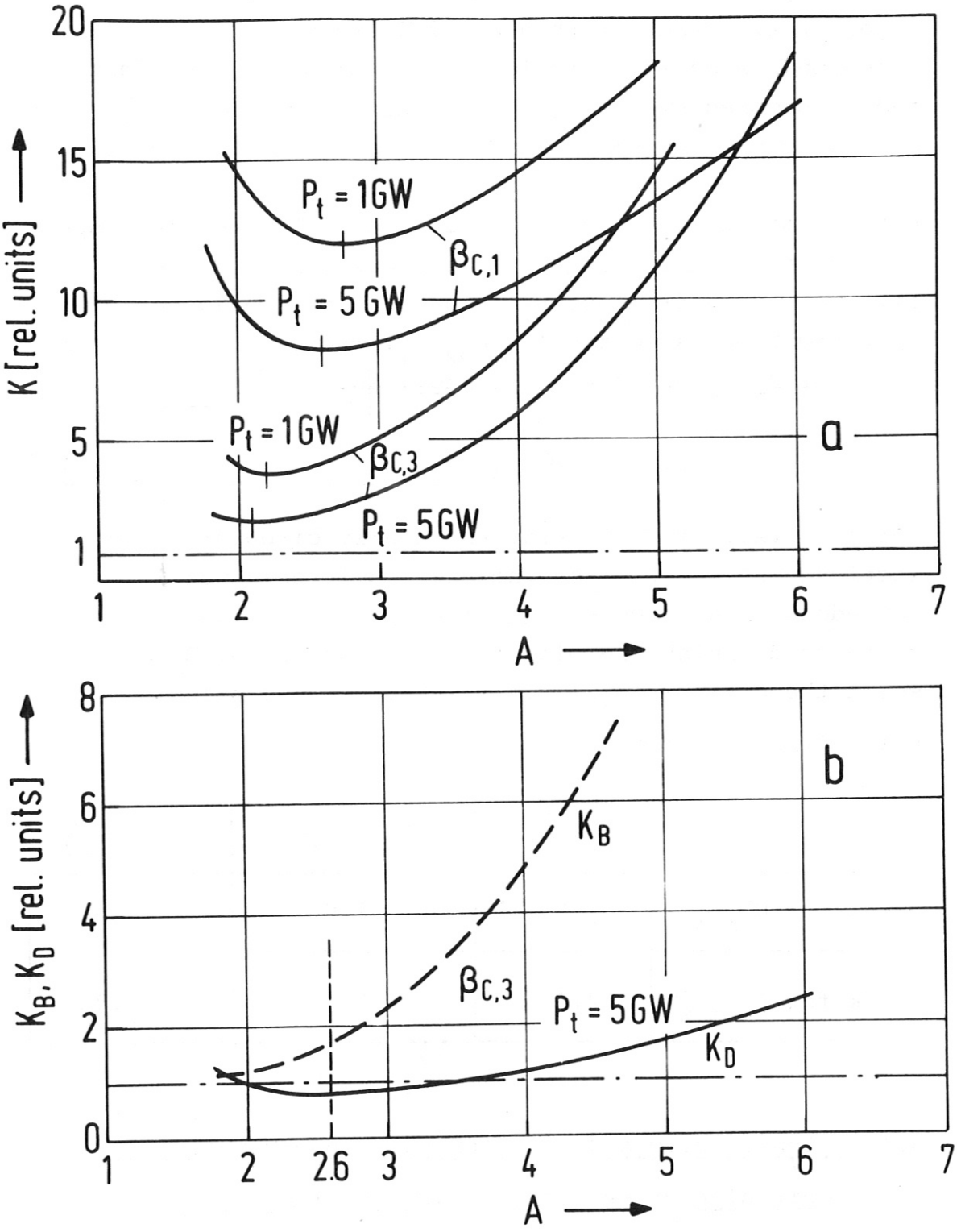

Fig. 7 a) Magnet and blanket costs K, as function of A relative to standard reactor costs, for two β_c given in Fig. 6 and for P_t = 1 GW and P_t = 5 GW.

b) Cost split for $\beta_{c,3}$; P_t = 5 GW,
K_B = rel. magnet costs; K_D = rel. blanket costs

Generally there is no substantial advantage, if any, when aspect ratios smaller than A = 2.5 are chosen. A = 3 is a reasonable choice. For lower reactor power the plasma radius becomes smaller (e.g. between 4 to 8 m for P_t = 1 GW) and the cost minimum is shifted to slightly higher A.

For optimizations of costs it is useful to know the aspect ratios where a minimum of E^* or a maximum of P_w, for different $\beta_c = f(A)$, occurs. A good, numerically tested approximation is to express $A_{extr.}$, where either extrema of E^* or of P_w occur (for B-scaling), as:

$$A_{extr} = k \left(\mathcal{R} + \frac{D}{a}\right) \qquad (27)$$

which is valid for circular and nearly circular cross sections. The position of the extrema is only weakly dependent on "a" since $\frac{D}{a} << \mathcal{R}$. Thus parameters which for instance diminish the plasma radius, as P_t, β, B_m etc., shift the optimum $A_{extr.}$ to slightly higher values.

k is given as follows:

	$\beta_c \sim \frac{1}{A}$	$\beta_c \sim \frac{1}{A^{3/2}}$	$\beta_c \sim \frac{1}{A^2}$
k for E^*_{min}	1.9	1.6	1.4
k for $P_{w\ max}$	2.5	2.2	1.85

3.1.3 Sensitivity analysis for various parameters at circular cross section for B-scaling

To get an idea on the sensitivity of the scaling results for the so far unvaried parameters it is useful to express the E^*, P_w, and the associated costs by power functions of those parameters. Those unvaried parameters are $\mathcal{R}$, D, f_p, τ . So we get for example $\frac{E^*_2}{E^*_1} = \left(\frac{\mathcal{R}_2}{\mathcal{R}_1}\right)^{\alpha}$ with all other

parameters fixed. This procedure is possible since it turned out that in log-log plots the variables vs. E^* or vs. P_w gave nearly straight lines over an appreciable range. This sensitivity analysis was done at beta values of β_o = 2 % and β_o = 10 %, for P_t = 5 GW and B_m = 8 T, at A = 3. The results are given in table 3 in a self explanatory manner:

Table 3

		E^*	P_w	range
		exp.	exp.	
β_o = 0,02	$\mathcal{R}$	3	-2.95	$1.1 < \mathcal{R} < 1.3$
	D	0.35	-0.3	$1 < D < 2.5$ [m]
	τ	0.86	-0.6	$0.2 < \tau < 1$
	f_p			$0.1 < f_p < 1$
β_o = 0,1	$\mathcal{R}$	2.5	-2.9	
	D	0.87	-0.65	see above
	τ	0.77	-0.5	
	f_p			

Example:

If E^*_1 and Pw_1 are taken at β_o = 0,02, we get:

$$\frac{E^*_2}{E^*_1} = \left(\frac{\mathcal{R}_2}{\mathcal{R}_1}\right)^3 ; \quad \frac{P_{w2}}{P_{w1}} = \left(\frac{\mathcal{R}_2}{\mathcal{R}_1}\right)^{-2.95}$$

It turns out that the scaling is extremely sensitive against variation of $\mathcal{R}$, but the reasonable range is low. In other words the reacting plasma should be as close as possible at the first wall. Thick separation sheaths (gas blankets, divertor sheaths etc.) are expensive. The overall blanket thickness has relative low influence as long as $D < \mathcal{R} \cdot a$ for low β.

3.2 Parameter scaling for strongly elongated cross sections

An overview on the parameter space for 5 GW reactors with various aspect ratios and standard parameters (B_m = 8 T), but with an elongation $\varepsilon = 4$, is shown in Fig. 8. The plot is equivalent to Fig. 5 for circular cross section. Since for strongly elongated cross section there is not sufficient information on stability, only the conventional scaling (21) with $q_a \approx 3$ and $\beta_p = A/3$ is indicated. The core constraint is computed for air core, according to 2.2.1, and $f_p = 0{,}5$ is assumed.

Contrary to circular cross section the optimum β_c values cannot be reached. The core constraint is a leading constraint and Y-scaling is appropriate. Then obviously the aspect ratio cannot be chosen freely but a certain combination of A and P_w or of A and a (see equ. (9)) is determined by the scaling, if optimum parameters shall be achieved.

Comparing the circular cross section at B_m = 8 T and the $\varepsilon = 4$ cross section each at conventional scaling (i.e. for the same q_a) it turns out that the magnetic energy and the blanket volume can be reduced typically by a factor 10. Wall loading of about 3 MW/m^2 and plasma radii of 2 m should be obtained at $\varepsilon = 4$.

More detailed features of Y-scaling with $\beta_{c,1}$ are given in the next figs. 9, 10. The mutual dependence of reactor parameters is now very different from that obtained at circular cross section with B-scaling. Because the stability assumptions are not well founded the quantitative results should be considered with caution, but the qualitative features of the interaction of core constraint and a typical $\beta_c \sim \frac{1}{A}$ may be instructive.

Fig. 9 (ε = const = 4; $E^* = E^*(A)$; parameter: P_t, and Iso-P_w-curves) shows that E^* is not very sensitive against variation of A for a fixed P_t. There is even a flat minimum in E^* for values of B_m smaller than 8 T. So working

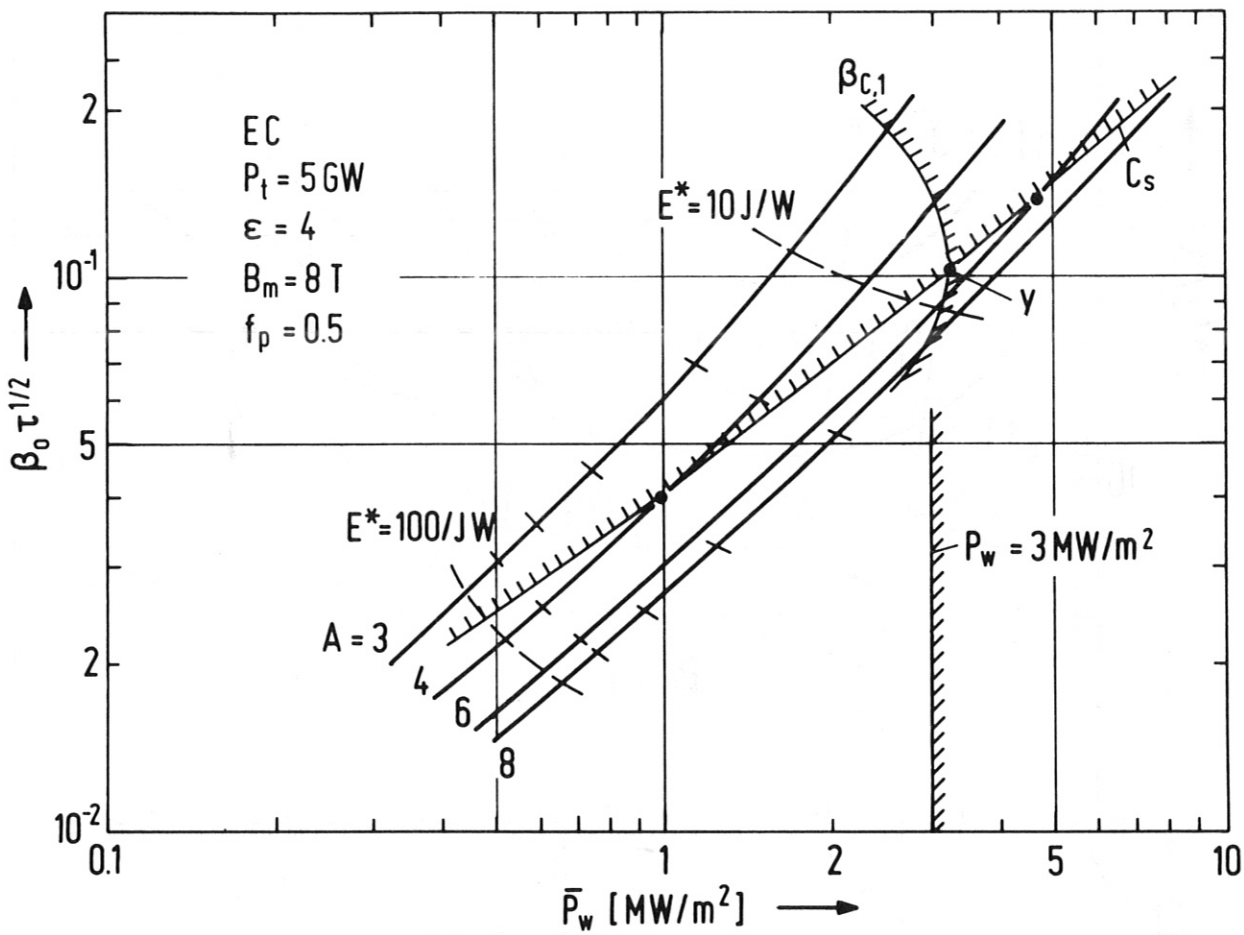

Fig. 8 Working range for 5 GW(th) tokamak reactors with elongated cross section, ε = 4.
B_m = 8 T; f_p = 0.5; C_s for ΔB = 16 T, η = 2,
q_a/q_o = 3; $\beta_{c,1}$ for β_p = A/3 and q_a = 3.

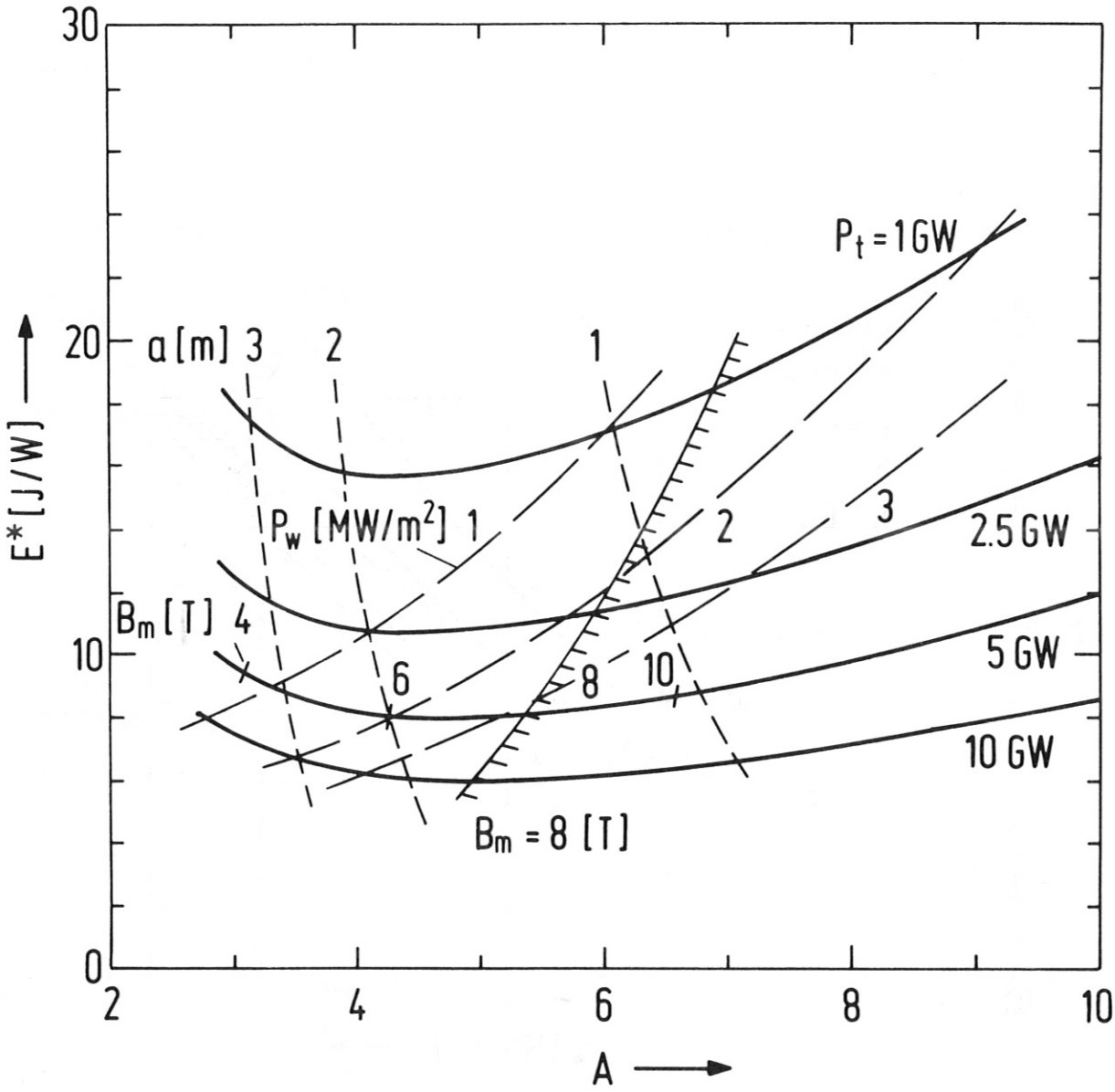

Fig. 9 Magnet Energy E* vs. aspect ratio A, limited by $\beta_{c,1}$ and C_s (Y-scaling of Fig. 5c). $\beta_{c,1}$ with $\beta_p = A/3$ and $q_a = 3$; $B_m = 8$ T.
Parameter: P_t = thermal reactor power
P_w = wall loading
a = small plasma semi axis
Elongated cross section, $\varepsilon = b/a = 4$.
(For $P_t = 5$ GW various B_m are indicated)

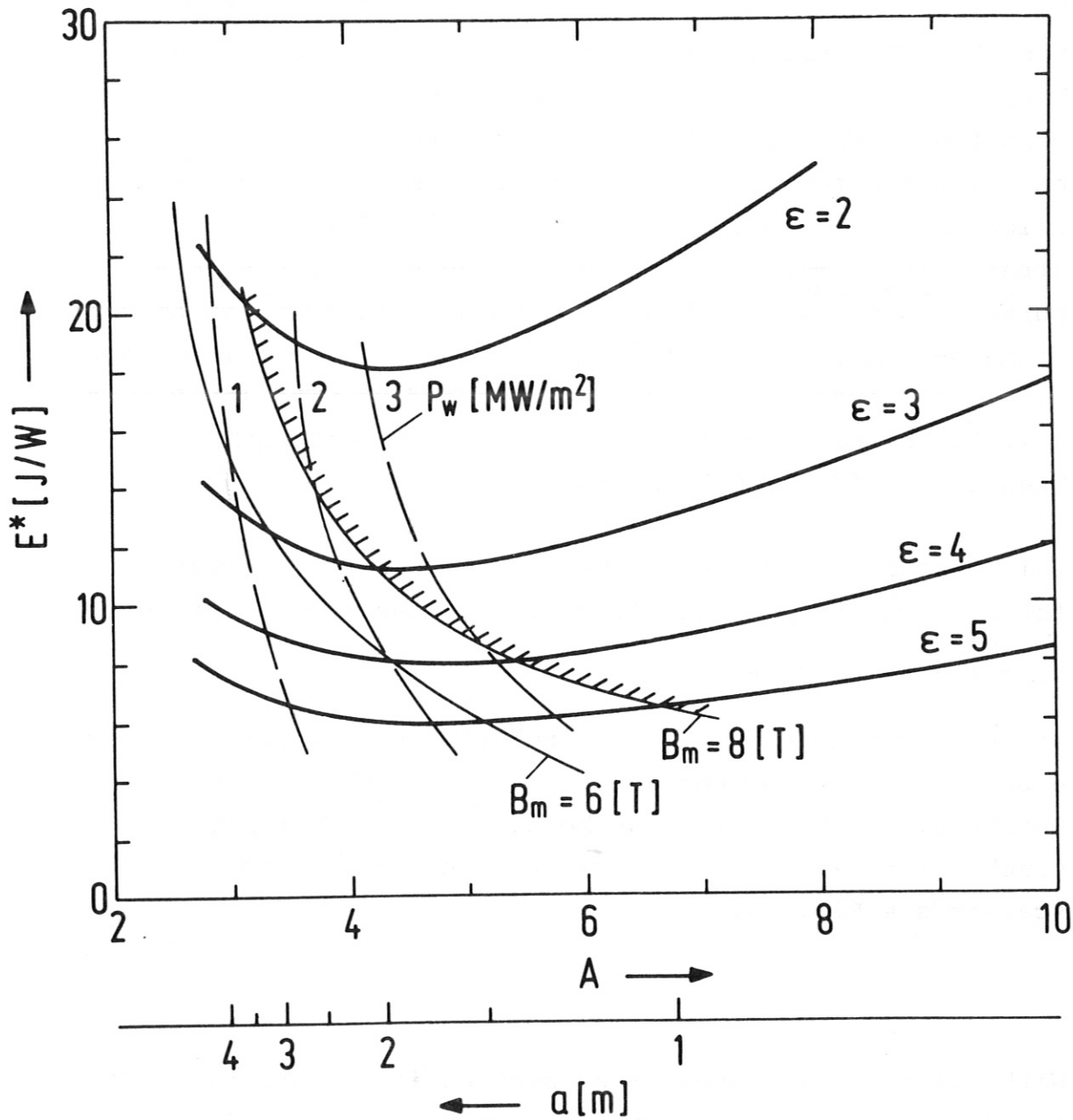

Fig. 10 E* vs. aspect ratio A, as in Fig. 9; P_t = 5 GW.
Parameter: ε = b/a
Elongated cross section
The abszissa a [m] is approximately valid for all ε.
It is exact for ε = 4.

at $B_m < 8$ T may even save costs, provided that P_w is limited. Going from a 1 GW to a 10 GW reactor there is approximately a factor 3 reduction in E_B^* and V_D^*.

The effect of ε-variation at constant P_t is demonstrated in Fig. 10. The improvement in the economy parameters with higher ε becomes increasingly lower beyond $\varepsilon = 5$. There are competing effects: Primarily we have the favourable $\beta_c \sim \varepsilon^2$, but with increasing ε the plasma radius becomes smaller, which in turn enforces larger A to fulfill the core constraint ($\beta_c \sim \frac{\varepsilon^2}{A}$). Additionally, staying on the $B_m = 8$ T curve we get a $\gtrsim$ D at higher ε, and a relative high amount of magnet energy is wasted in the blanket. But following a P_w = const curve toward higher ε we end up with low B_m, to fulfill the core constraint via larger radial dimensions. Then $E^* \sim 1/(\beta^2(\varepsilon)\ B_m{}^2)$ applies.

This features of strong elongation do not change very much for $\beta_c \sim \frac{1}{A^2}$ or $\beta_c \sim \frac{1}{A^{3/2}}$ if only the reasonable restriction $B_m \lesssim 8$ T is observed.

So in this scaling with $\beta_{c,1}$ a relative high improvement of economy factors for reactors is achieved by the elongation. Reasonable upper limits may be at $\varepsilon = 5$ to 7 (cf. belt pinches work at $\varepsilon = 10$ to 30). For an approximate cost scaling see Fig. 18.

With strongly elongated cross section it is possible that the β value given by plasma physics surpasses a limit which is set by other constraints. So the obvious question is: What are the limiting optimum reactor parameters given only by the technological constraints, namely P_t, B_m, core constraint and maximum wall loading? This question is answered by P-scaling, see Fig. 5c, in a very general diagram (Fig. 11) for $\varepsilon = 4$, 5 GW-reactors,

parameter: B_m, A and Iso-E*. Note that $\beta' = \beta_o \cdot f_p^{1/2} \cdot \tau^{1/2}$ is an independent parameter, there is no prior specification of β' by plasma physics. The core constraint is given for plasma currents consistent with $q_a/q_o = 3$. The construction of this diagram can be traced back to Fig. 8. The diagramm contains the points P of Fig. 5c but now for various B_m. For comparison we include an adequate diagram (Fig. 12) for circular cross section. Again, this diagram should only be interpreted if P_w and C_s are leading constraints, which at best can be expected for high-ß-equilibria.

An interesting feature shows up when cross sections with various elongations are compared with circular cross section in P-scaling, but with the same parameters P_t, Bm, f_p, D, $\mathcal{H}$ (Fig. 13). Obviously the elongated cross sections give for a fixed β_o value and for increasing ε substantially lower E^* and V_B^*. The effect saturates at $\varepsilon = 6$ and even reverses for higher ε. This purely geometrical effect comes about because in strongly elongated cross sections relatively more plasma is situated in a region with high magnetic field and because $P_t \sim B^4$. Whether this feature will hold in reality remains to be seen. It would be necessary to have vertically (along b) stretched inner flux surfaces and favourable vertical pressure profiles. Note, that in our rough treatment the vertical properties of the elongated plasmas are rather pessimistically specified by $\frac{bw}{b} = \mathcal{H}_b = \mathcal{H}_a$ and by $f_{p,EC} = f_{p,CC}$ only.

3.3 FCT-equilibria with circular and nearly circular cross section

As outlined in /22/, FCT equilibria for high-ß exist only with relatively steep pressure profiles in a narrow range of pressure profile halfwidths (HW) between .4 and .55. Thus the scaling considerations should be made under the constraint of a fixed pressure profile. Since in the FCT equilibria high ß and consequently high densities and high burn up fractions may be achieved, the influence of α-particle pressure and of specific temperature and density distribution have to be discussed.

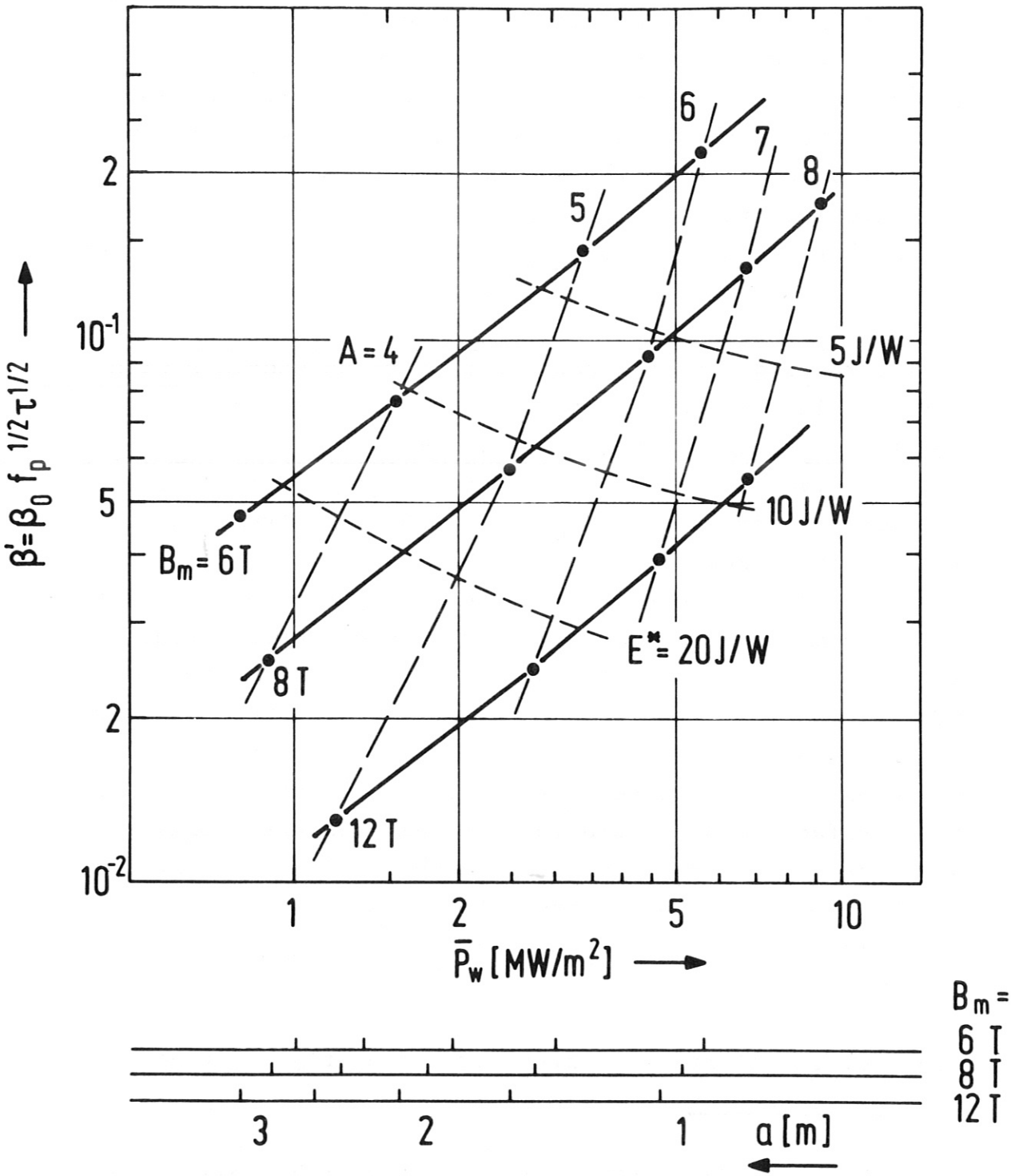

Fig. 11 Working range for 5 GW(th) tokamak reactors with elongated cross section, $\varepsilon = 4$.
P_w and C_s are leading constraints: P-scaling (see Fig. 5c); C_s for $\Delta B = 16$ T, $\eta = 2$, $q_a/q_o = 3$.

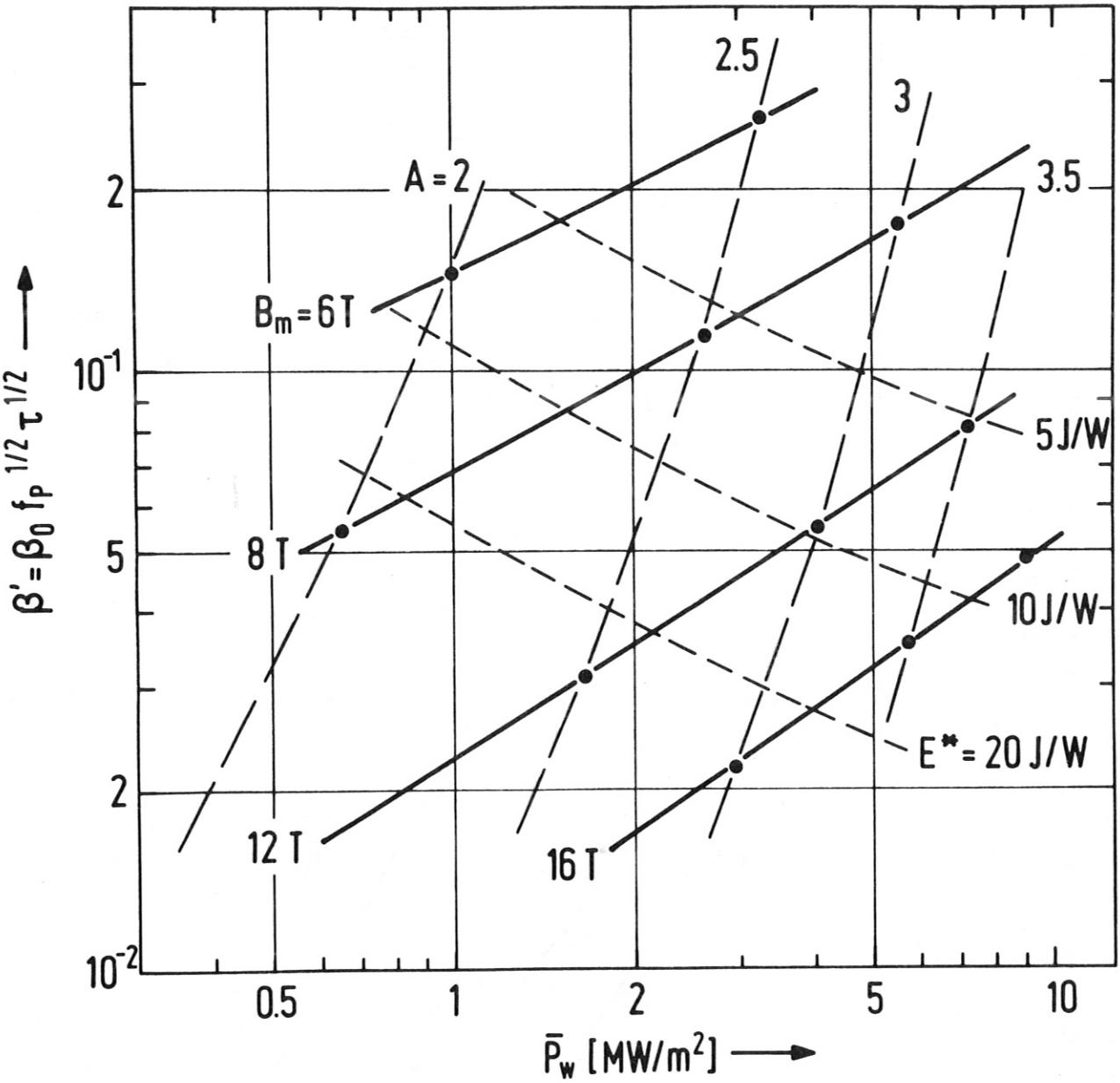

Fig. 12 P-scaling for 5 GW(th) tokamak reactors as in Fig 11 but for circular cross section.

Fig. 13 Wall loading (left) and toroidal magnetic field energy (right) vs. β_o, determined by C_s (ΔB = 16 T; η = 2; q_a = 3) and P_w for 5 GW(th) reactors with circular and elongated cross section (ε = 2 ÷ 5). P-scaling. The numbers on the curves refer to the aspect ratio necessary.

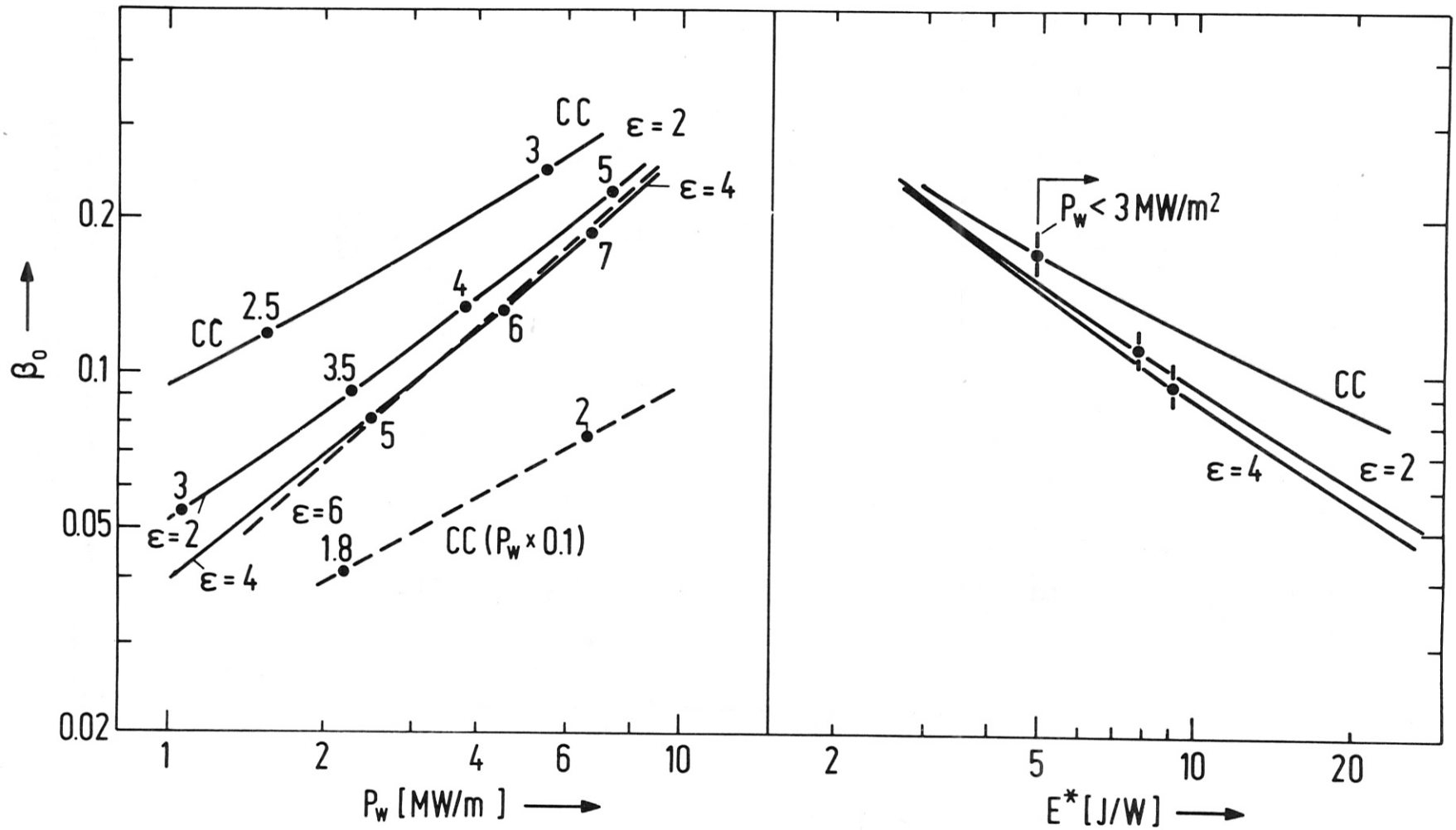

3.3.1 n(r) and T(r) distribution within a given pressure profile

Profiles of the form $n = n_o\,(1-(\frac{r}{a})^2)^{\nu}$ and $T = T_o(1-(\frac{r}{a})^2)^{\delta}$ were assumed, including the condition that $n \cdot T$ matches a given pressure profile, which is adequate to FCT-profiles (e.g. $p(r) = (1-(\frac{r}{a})^2)^{5/2}$ with HW $\approx$ 0,5 and $n_o \cdot T_o$ = const).

The following relative $\bar{Q} = V_p^{-1} \int Q\, dv$ (Q = power density)

with $Q = \frac{n_i^2}{4} \langle \sigma v \rangle\, Q_T = \frac{1}{4} n_i^2(r) \exp(-\frac{19.9}{T_{i(r)}^{1/3}})\, T_i^{-2/3}(r) \cdot Q_T$

are obtained:

δ	ν	$\bar{Q}$,rel T_o = 15 keV	$\bar{Q}$,rel T_o = 30 keV
0	2.5	1	1
2.5	0	0,96	1,17
1.25	1.25	0,93	1,14

Obviously the $\bar{Q}$ don't depend very much on the detailed structure of the (nT) profiles. This was to be expected because the power production is localized in the plasma center, where n and T do not change very much with radius, or where $\frac{\langle \sigma v \rangle}{kT^2}$ (for fixed pressure) is approximately constant. Accordingly only (nT) need to be specified for this study. Also the question about compatibility between T- and q-profiles is not relevant here /30/.

3.3.2 Influence of α-particle pressure

The effects of α-pressure are discussed only for the central plasma region, $(nT)_o$, where the fusion power density is high (see Fig. 14). The broadening of the source profile due to α-drift orbits is small /32/ and is neglected.

The α-pressure is given by:

$$p_\alpha = n_\alpha T_i + \frac{2}{3} n_\alpha' \bar{E}_\alpha$$

where the second term is the pressure of α-particles thermalizing at any time, with a mean energy $\bar{E}_\alpha$. The α-particle densities shall be given by the α-production rate times the α-containment time $\tau_{c,\alpha}$, or the slowing down time $\tau_{s,\alpha}$. So we get:

$$\frac{p_\alpha}{p_e+p_i} = \frac{n_i^2 \langle\sigma v\rangle}{8 \cdot T \cdot n_i} (T_i \tau_{c,\alpha} + \frac{2}{3} \bar{E}_\alpha \tau_{s,\alpha}) \qquad (28)$$

where $$\tau_{s,\alpha} \approx 10^{13} \cdot T_e^{3/2}/(\ell n \lambda \cdot n_e) \text{ [sec]};[\text{kev, cm}^{-3}] \qquad (29)$$

The physics of α-particle containment is not well known. Düchs and Pfirsch /32/ treat the production, thermalization and neoclassical diffusion of α-particles in a tokamak plasma. For a background plasma with fixed parameters (T_o = 20 keV, $n_o = 10^{20}$ m^{-3}, parabolic profile), which is essentially a reactor situation, they found, for burn times up to 30 sec, negligible α-diffusion with $\tau_{c,\alpha} > 100$ sec. Correspondingly they got a continuous built-up of α-pressure. (Their n_α and n_α' for α's with $E_\alpha \geq 150$ keV) agree well with those obtained by the rough formulas (28) and (29).

So the burn time τ_b of a reactor may be limited either by

a) the built-up of α-pressure in the plasma center and by the associated deformation of the pressure profile. or by
b) the reduction of reactor power if the total pressure is held fixed.

The burn time for the two cases can roughly be estimated, if the central plasma temperature is fixed, which means that the local energy deposition by the α's is quickly carried outward by energy transport processes ($\tau_E < \tau_{c,\alpha}$). An additional active control mechanism would surely be necessary. Since the plasma would burn at optimum temperature the estimates are optimistic.

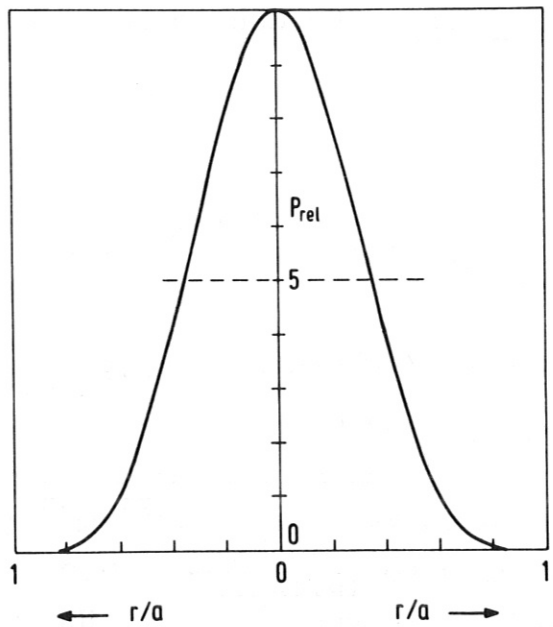

Fig. 14 Normalized fusion power density profile for $n = n_e(1-(\frac{r}{a})^2)^{2.5}$ and T_o = const.

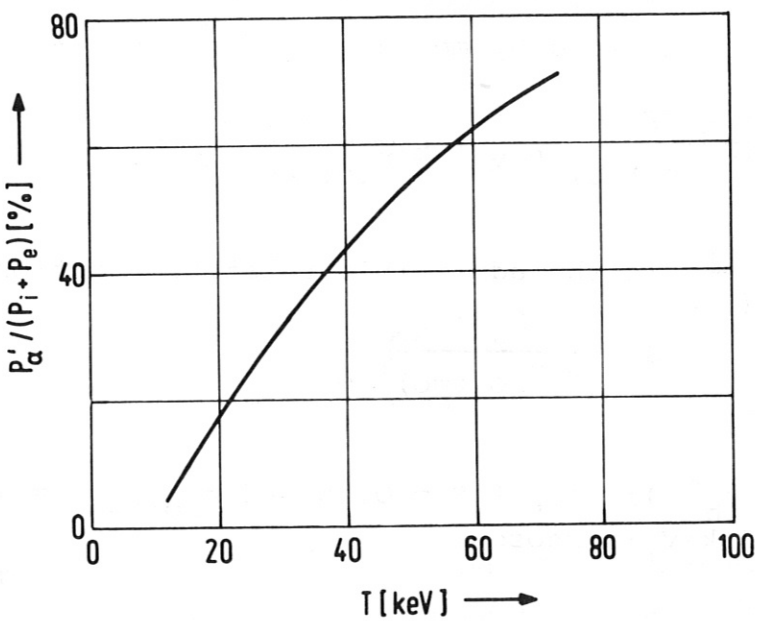

Fig. 15 Relative α-particle pressure of thermalizing α-particles as function of the plasma temperature according to equ. (33)

a) Fixed central background plasma parameters $T_o = T_i \doteq$ $= Te_o = \text{const}$, $n_{io} = \text{const}$ (by controlled fuelling).

The pressure limited burn time is deduced to be approximately:

$$\tau_b \approx \frac{p_\alpha}{(p_e+p_i)_{t=o}} \frac{8}{n_{io} \langle\sigma v\rangle} - \frac{2}{3} \frac{\bar{E}_\alpha \cdot \tau_{s,\alpha}}{T_{io}} \quad [\text{sec}] \qquad (30)$$

$\bar{E}_\alpha$ can be taken from /33/ where $\bar{E}_\alpha = \frac{E_\alpha}{\ell n(E_\alpha/E_c)}$ and: $E_\alpha = 3.52$ MeV, $E_c = 32\ T_e$.

For example if: $T_{io} = 15$ keV; $n_{io} = 10^{21}\ m^{-3}$ (FCT equil.) and we allow p_α to grow to $\frac{p_\alpha}{(p_i+p_e)_{t=o}} = 1.0$, which gives roughly a 15 to 20 % shrinkage of HW, we get: $\tau_b \approx 15 - 2.8 \approx 12$ sec. An increase of B to $1.4 \cdot B_{(t=o)}$ would be necessary too.

b) Fixed total central plasma pressure $p_e + p_i + p_\alpha =$ $= \text{const} = (p_e + p_i)_{(t=o)}$; $T_o = \text{const}$.

The burn time is now limited by the reduction of the power output during the pulse. The appropriate density n_i shall be maintained by means of refuelling. We get:

$$\tau_b \approx \frac{4\ (1-G-\sqrt{R})}{\sqrt{R}\ (1-G) n_{i\ o(t=o)} \langle\sigma v\rangle} \approx \frac{4\ (1-\sqrt{R})}{\sqrt{R}\, n_{io(t=o)} \langle\sigma v\rangle} \qquad (31)$$

Where $R = \frac{R'(t)}{R_{(t=o)}}$ is the admissible relative reaction rate and $G = \frac{2}{3} \frac{\bar{E}_\alpha \cdot \tau_{s,\alpha}}{n_{io(t=o)} T_{io}}$

For example $\tau_b \approx 15$ sec, if $R = 0.25$, and $n_{io(t=o)} = 10^{21}\ m^{-3}$, and $Ti_o = 15$ keV, is chosen.

The burn time limitation is particularly severe for the high ß- or FCT-equilibria because in both cases a) and b) $\tau \sim \frac{1}{n_{io}} \sim \frac{1}{\beta_o}$. In reality difficulties in controlling the temperature profiles (thermal stability) may arise.

With burn times in the 10 sec range and recharge times of at least 100 to 200 sec (taken from reactor designs) the duty time becomes $\tau = 0.1 \div 0.05$. The capital costs for magnetic field and blanket scale in the FCT-parameter range like $K \sim \tau^{-0.64}$. So from Fig. 16 (below) we get costs for the burn time limited cases which are close or somewhat higher than those of the standard reactor (see Fig. 18).

There is some hope that the α-particles are carried outward together with the fuel ions by local instabilities (e.g. sawtooth relaxation) or by coarse turbulence. Then $\tau_{c,\alpha} \approx \tau_{c,i}$ can be assumed and equation (28) applies. With a fuel burnup given by $f_b \approx n_i T_i \frac{\langle \sigma v \rangle}{2}$ we receive:

$$\frac{p_\alpha}{(p_i+p_e)} = \frac{f_b}{2} + \frac{p_\alpha'}{(p_i+p_e)} \qquad (32)$$

The second term, which is the relative pressure of the thermalizing α's, is strongly temperature dependent /33/. For Ti = Te we get:

$$\frac{p'_\alpha}{(p_i+p_e)} \approx \langle \sigma v \rangle \, T_i^{1/2} \, \bar{E}_\alpha \cdot 10^{13} \quad \text{(in keV; cm; sec)} \qquad (33)$$

This relation is plotted in Fig. 15. Obviously, in a long pulsed reactor plasma high central temperatures must be avoided. For a Ti_o = 15 keV plasma and a burn-up of 10% a fractional α-pressure of about 15 to 20 % has to be expected.

3.3.3 Approximate working range for FCT-reactors

In Fig. 16 the position of FCT equilibria in our standard diagram (cf. Fig. 5) is depicted. Two examples /22/ F_1 and F_2 are marked, where we have transposed for the purpose of scaling the numerically obtained assymmetric profiles to roughly adequate symmetric profiles with circular cross section, according to 2.1.

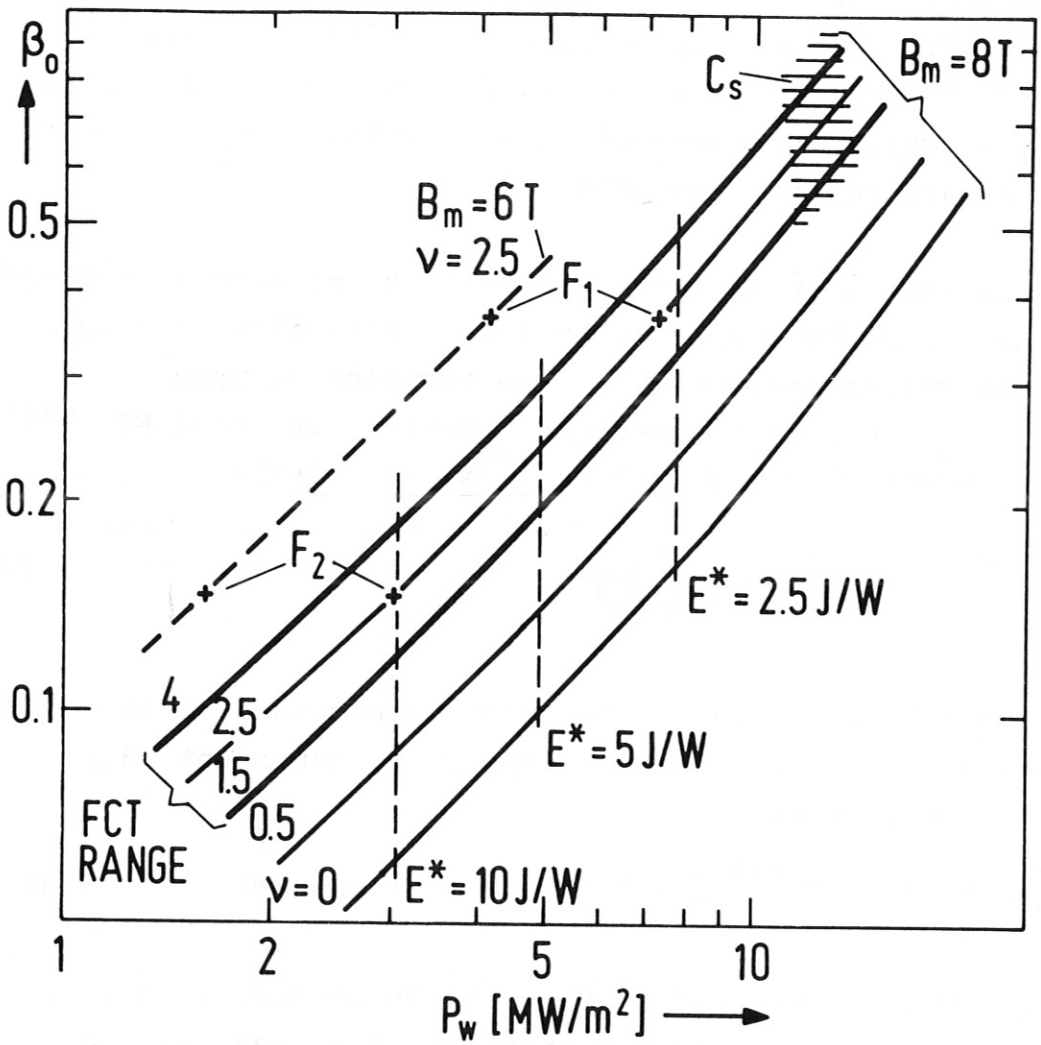

Fig. 16 Approximate working range for 5 GW(th) tokamak reactors for high-ß (FCT) equilibria with nearly circular cross sections.
Profiles: $n = n_o(1-(\frac{r}{a})^2)^{\nu}$; T_o = 15 keV;
Parameter: ν;
F_1 : ß = 10.7 %; HW = 0.5
F_2 : ß = 4.2 %; HW = 0.5 according to /22/
An approximate working range for FCT at B_m = 8 T and for a pressure profile half width 0,4 ÷ 0,6 (ν = 4 ÷ 1.5) is indicated.

Fig. 16 shows the influence of the profile factors or of the pressure profile HW. For typical FCT situations ($\nu \approx 2.5$) the central ß values have to be about a factor 2 higher, to be competitive with the standard profiles, provided we achieve the same pulse time in both cases (note: the iso-E^* lines match P_w = const.). Nevertheless, if the numerically calculated equilibria with mean ß values of 10.7 % resp. 4.2 % could be stably maintained, quite substantial economic advantages would accrue. For a rough cost comparision see Fig. 18. As roughly indicated in Fig. 16, the core constraint would not be limiting for A = 4. The high Pw for Bm = 8 [T] even suggests to work at lower magnetic field, for example at 6 [T], which does not enlarge the costs very much (Fig. 18).

4. ESTIMATE OF RELATIVE COSTS

This parameter study allows only a very crude comparative cost estimate for the magnet and for the blanket + shield. The procedure is explained in 3.12. Since the reactor formats for the different plasma shapes (CC; EC; slightly elongated FCT) may be different too, cost comparisions between them are very speculative. We chose here B_m = 8 T for all designs, so at least the costs evaluate essentially volumina only.

Fig. 17 shows the sum of relative blanket + magnet costs for standard reactor parameters with circular cross section. The range of cost variation may be limited by the indicated constraints. From the Fig. 17 it can be derived that the costs scale for $ß_o$ between 1 and 3 % ($0.7 < ß < 2$ %) as $K \sim ß_o^{1.6} \cdot \tau^{-0.8}$ and for $ß_o$ between 8 and 15 % ($5 < ß < 10$ %) as $K \sim ß_o^{1.25} \cdot \tau^{-0.62}$; both are taken at A = 2,5 and B_m = 8 [T]. For elongated cross section the cost comparision is done with the same assumptions as for CC. To select design parameters Y-scaling with $ß_{c,1}$, but for two different q_a (q_a = 2.5 and q_a = 3.5; $ß_p = \frac{A}{3}$) and for various ε_i is applied (Fig. 18). Included in the plot are

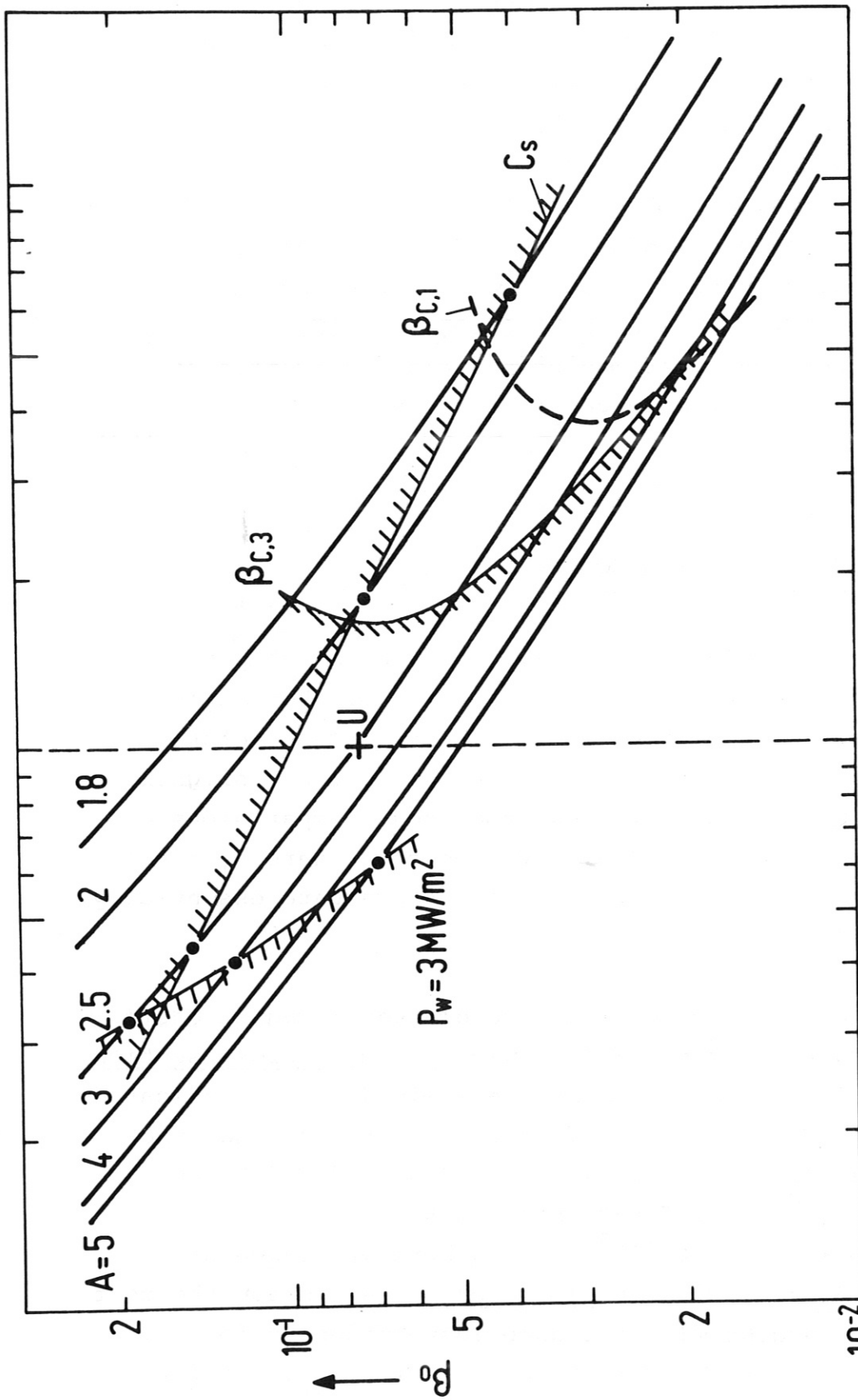

Fig. 17 Costs for magnet and blanket, relative to those of a standard reactor U (see tab. 4). Circular cross section; $B_m = 8$ T; $f_p = 0.5$; $\tau = 1$.

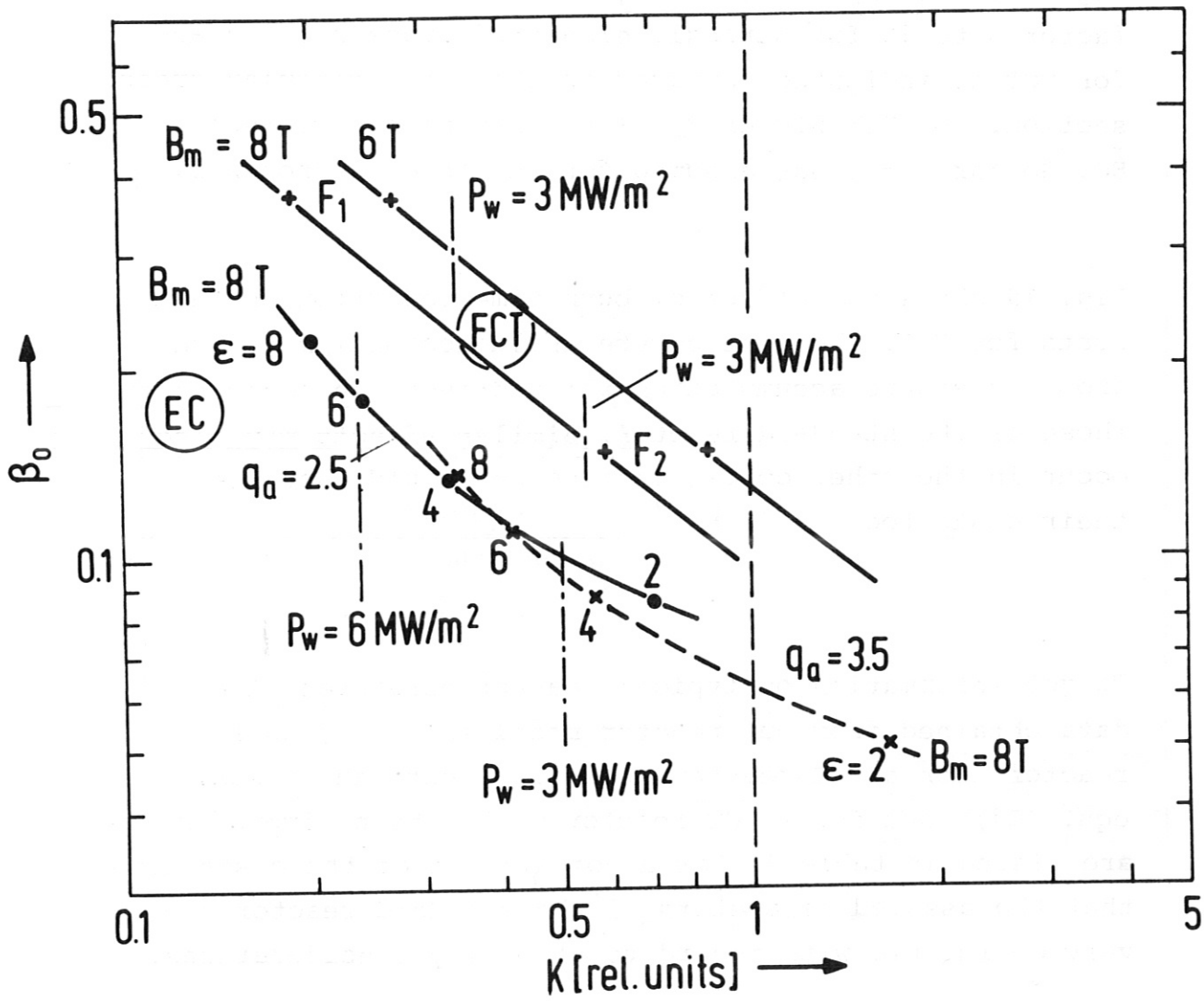

Fig. 18 Relative costs as in Fig. 17 for FCT (F_1 and F_2 are the two examples of Fig. 16) and for elongated cross section (EC) with various ε. For EC the indicated points are determined by $\beta_{c,1}$ (with $\beta_p = A/3$; $q_a = 3.5$ and $q_a = 2.5$) and by the core constraint C_s at $B_m = 8$ T (Y-scaling). $P_w = 3$ MW/m² is indicated at all curves.

the cost estimates for "FCT reactors" with the two configuration examples F_1 and F_2. Roughly a cost saving of a factor 3 to 10 for strongly elongated cross sections and for FCT is indicated, compared to those for circular cross section. For FCT higher β_o-values are necessary than for EC. So far, τ = 1 was assumed for the three approaches.

Fig. 19 shows the effect of burn time reduction on the costs for FCT. The most severe influence on τ may come from α-pressure accumulation which drives the costs beyond those of the standard reactor. Similar effects may also occur in the other configurations and would increase their costs too.

To get information on typical reactor parameters the data obtained from our reactor model for the standard reactor, for an EC reactor (ε = 3, conventional β-scaling equ. (21)) and for a FCT reactor with a burn time of 200 s are listed in table 4. For a comparision of the costs note that the assumed parameters of the standard reactor are very optimistic with regard to stability considerations.

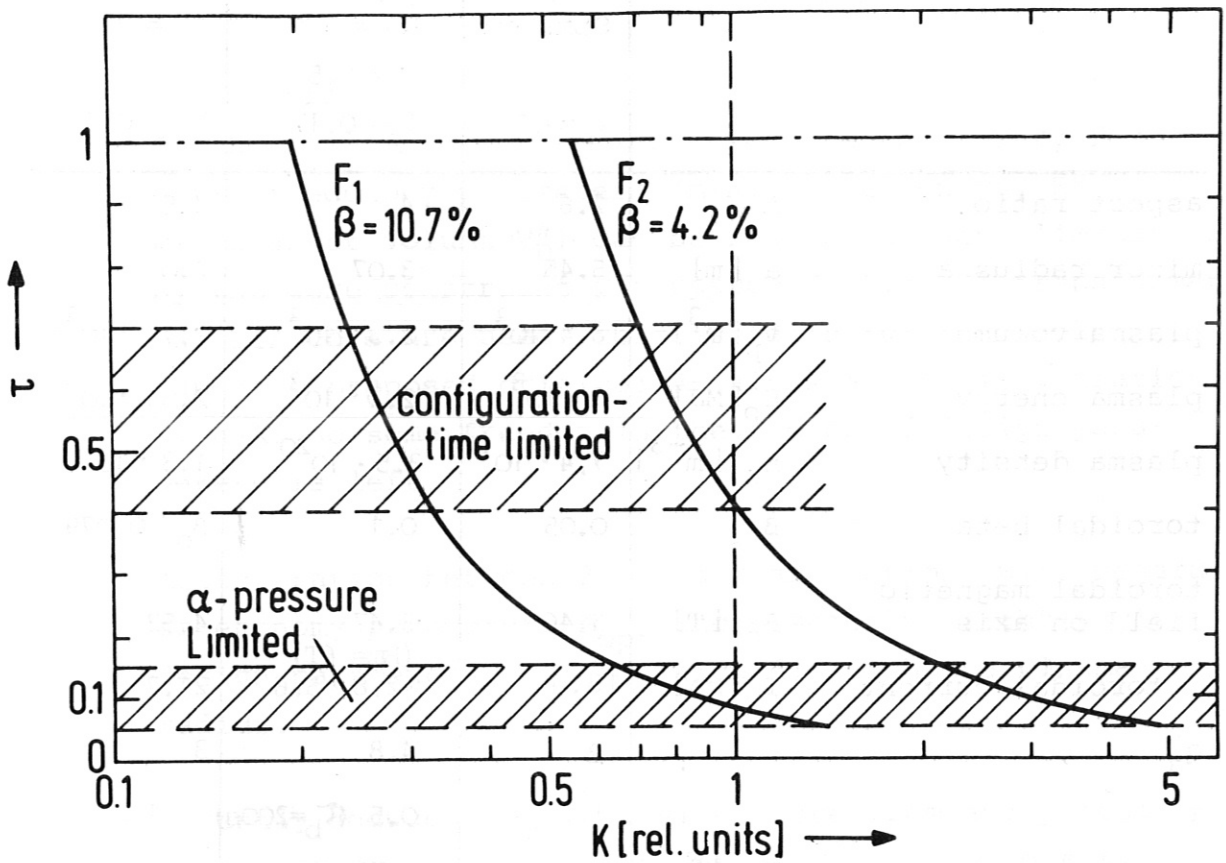

Fig. 19 Relative magnet and blanket costs, K, for "FCT reactors" dependent on the duty factor τ (burn time to cycle time). Approximate regions of possible τ-limitations are indicated by the hatched areas.

Table 4 Representative data of 5 GW reactors.
(T_i = 15 keV; $\mathcal{M}$ = 1.2; D = 1.5 m, B_m = 8 T;
P_t = 5 GW; τ = 1; H = 1.5 m)

		C C Standard f_p=0.5	F C T Bm = 6 T HW= 0.5 f_p= 0.17	E C ε = 3 f_p = 0.5
aspect ratio	A	2.6	4	4.5
minor radius a	a [m]	5.45	3.07	2.0
plasma volume	V_p[m^3]	$8.4 \cdot 10^3$	$2.3 \cdot 10^3$	$2.71 \cdot 10^3$
plasma energy	E_p[MJ]	$3 \cdot 10^3$	$2.3 \cdot 10^3$	$2.55 \cdot 10^3$
plasma density	n_o [m^{-3}]	$7{,}4 \cdot 10^{19}$	$3.5 \cdot 10^{20}$	$1.3 \cdot 10^{20}$
toroidal beta	ß	0.05	0.1	$ß_o \approx 0.079$
toroidal magnetic field on axis	B_o [T]	3.46	3.47 (Bm= 6T)	4.52
toroidal current	I [MA]	18.4	∿2.8 → 5.6	21.7
q_a		2	4.8	3
τ		1	0.5 (τ_b=200s)	1
wall loading	$\bar{P}_w$[$\frac{MW}{m^2}$]	1.36	2.8	2.35
mean fusion power density (plasma) P_t/V_p	Wp [$\frac{MW}{m^3}$]	≈ 0.6	≈ 2.17	≈1.84
spec. magn. energy inside tor. coil	E^* [$\frac{MJ}{MW}$]	17.3	6.21	12.16
spec. blanket volume	V_D^* [$\frac{m3}{MW}$]	1.23	0.645	0.74
rel. magnet costs	K_B	67.5	22.5	44.0
rel. blanket + shield costs	K_D	32.5	19.7	22.5
rel. total core costs	K	100	42.2	66.5

5. CONCLUSIONS

Within the uncertainties of basically realistic to optimistic assumptions the parameter study yields information for long time pulsed, 5 GW_{th} tokamak reactors, as follows.

1) Circular cross section.
   - For $B_m \leq 10$ T aspect ratios which are neccessary for optimum economy parameters (min. magnet energy E^*, min blanket volume V_D^*) can be reached without limitations by the core constraint if superconducting OH transformer and air core are used. This is valid for the whole range of proposed critical ß-values and their variation with A. So some freedom in the choice of design parameters is left.

   - Aspect ratios between 2.5 and 3 are optimal with regard to economy parameters. A_{opt} increases only slightly with design parameters (P_t; ß), which diminish the plasma radius.

   - Recently deduced $ß_c$ (inclusive those from analytical high-ß theory) lead to maximum ß values of 3 to 4 %, which are not sufficient to reach the economic features (E^*, V_D^*, associated costs) of a standard (UWMAK I) design.

   - Going from P_t = 1 GW to 10 GW about a factor 3 is gained in those economy parameters.

2) Elongated cross section, generally ε = 3 to 4, with conventional $ß_c$-scaling ($q_{a,EC} = q_{a,CC} = 3$) yields:
   - Aspect ratios of 4 to 5 are required to fulfill the core constraint. Air core and high bidirectional flux density swing (e.g. ΔB = 16 [T]) are necessary to achieve improved economy parameters.

- If the elongated and the circular cross section reactors are compared under equivalent conditions (same B_o = 8 T; same $\beta_{c,1}$-scaling), considerable improvements in the economy parameters can be achieved by the elongation, although A must be higher for EC. The magnetic energy and the blanket volume can be reduced by a factor 5 to 10, for ε of 3 to 4. Then P_w of about 2 - 3 MW/m^2 and a $\gtrsim$ 2 m are attained. If ε is varied, the economy parameters still improve with ε up to ε = 6 to 8, where a saturation occurs due to competing effects.

- The scaling with the core constraint and with β_ℓ shows: E^* is not sensitive to A-variation. Even B_m lower than 8 T may be economically advantageous, yielding slightly lower E^*, but reduced P_w.

- A B_m of 8 T (NbTi superconductor!) is sufficient to reach $P_w \gtrsim 3$ MW/m^2. For that purpose no higher β_o than 10 to 12 % is needed. An increase of B_m beyond 8 T would enlarge P_w only - to values possibly too high for a reasonable wall lifetime. But it would not lower the magnet energy. This is in contrast to the CC, where P_w's are attained which are presumably far too low. But at CC <u>all</u> economy parameters improve monotonously with increasing B_m (see Fig. 4).

- Since in race track cross sections with favourable vertical profiles, relatively more plasma is positioned at high magnetic fields than in circular cross sections, lower volumina and field energies for the same β_o can be achieved. This purely geometrical effect causes improvements of the economy parameters by a factor up to 2.5 for ε = 4, which saturate at ε = 5.

3) FCT.
Preliminary estimates using two examples of numerically calculated /2.22/ FCT equilibria, with reasonably steep current profiles, show:

- Economic advantages would accrue if long pulse times and the equilibrium limited ß-values could be achieved, although the fusion power production (α-particles) is mainly located in the plasma center, for the necessarily steep pressure profiles (HW = 0.5). If good α-containment is assumed, according to Düchs and Pfirsch / [32] /, α-pressure should limit the burn time to the 10 sec range, either by pressure profile deformation (FCT has profile sensitive equilibria) or by reduction of fusion power, for a profile in which the total pressure ($p_e + p_i + p_\alpha$) is held fixed. The reduction of burn time would lead to economy parameters and associated investment costs close to, or even worse than those of the standard reactor.

References:

1 Golovin I.N., Dnestrovsky Y.N., Kotomarov D.D.: Tokamaks as a possible fusion reactor - comparision with other CTR devices. Proc. Nucl. Fus. React. Conf., Culham, 194 (1969)

2 Stacey W.M., Evans K.: Toroidal field strength in tokamak reactors. ANL/CTR Technical Memo. No. 57 (1975)

3 Hatch A.J., Etzweiler J.: A simplified parametric study of tokamak fusion reactors. Technology of C.T. Fusion Exp. and Eng. Asp. of Fus. Reactors, Austin 755 (1974)

4 Kulcinski G.L., et al.: UWMAK-I. A Wisconsin fusion reactor design. Report UWFDM-68 (1973)

5 Knobloch A.F.: Technical limitation on conceptual tokamak reactors (part I). Proc. 6th Symp. on Eng. Probl. of Fus. Res., San Diego (1975).(Part II). Proc. 9th Symp. Fus. Techn. (SOFT) Garmisch-P. (1976)

6 Gruber O., Wilhelm R.: The Belt-pinch - a high ß tokamak with noncircular cross section. Nucl. Fus. 16, 243 (1976)

7 Furth H.P.: Tokamak research. Nucl. Fus. 15,487 (1975)

8 Spano A.H.: Large tokamak experiments. Nuc. Fus. 15, 909, 1975

9 Lubell, M.S.: ORNL-TM-4635 (1974)

10 Bünde R.: Cost sensitivity analysis of possible fusion power plants. To be published 1977

11 Gottlieb M.B.: Status of tokamak plasma physics. Rep. PPPL-1296 (1976)

12 Stacey W.M. et al.: Tokamak experimental power reactor studies. Report ANL/CTR 75-2 (1975).

13 Arendt F., et al.: Energetic and economic constraints on the poloidal windings in conceptual tokamak fusion reactors. Proc. 8th SOFT, Noordwijkerhout, 563 (1974)

14 Shafranov V.D.: Pressure limit of tokamak plasma. Fusion Reactor Design Problems, Culham, p. 249 (1974)

15 Freeman R.L. et al.: Doublet II A experiments. IAEA Conf. Berchtesgaden (1976), CN-35/A 10-3

16 Wesson J.A.: Hydromagnetic stability of tokamaks. 7th Conf. on Contr. Fus. and Plasma Phys., Lausanne 2, 102 (1975)

17 Callen J.D., Dory R.A.: "Magnetohydrodynamic equilibria in sharply curved axissymmetric devices. Phys. Fluids 15, 1523 (1972)

18 Peng Y.-K. M. et al.: MHD equilibria and local stability of axissymmetric tokamak plasmas. ORNL/TM-5267 (1976)

19 Becker G., Lackner K.: Equilibrium restrictions for elongated tokamaks. IAEA Conf. Berchtesgaden CN-35/B 11-3

20 Hoekzema J.A.: Toroidal equilibrium of noncircular sharp boundary plasmas surrounded by force free fields. 3rd Top. Conf. on Pulsed High Beta Plasmas, Culham, 535 (1975).

21 Callen J.D.: Tokamak plasma magnetics. IAEA Conf. Berchtesgaden (1976), CN 35/B10

22 Dory R.A., Peng Y.-K. M.: High pressure flux conserving tokamak equilibria. To be published Nucl. Fus. 1977

23 Clarke J.F., Sigmar D.J.: High-pressure flux-conserving tokamak equilibria. Phys. Rev. Let. 38,70 (1977)

24 Freidberg J.P., Haas F.A.: Kink instabilities in a high-ß tokamak with elliptic cross section. Phys. Fluids 17, 440 (1974)

25 Freidberg J.P., Grossmann W.: MHD stability of a sharp boundary model of tokamak. Phys. Fluids 18,1494 (1975)

26 Goedbloed J.P. et al.: Equilibrium and stability of high-ß tokamaks, screw pinches and belt pinches. IAEA Conf. Berchtesgaden (1976) CN-35/E22

27 Freidberg J.P., Goedbloed J.P.: Equilibrium and stability of a diffuse high-ß-tokamak. 3rd Top. Conf. on Pulsed High-ß Plasmas, Culham, 1975

28 Sigmar D.J.: High-ß tokamak. Proc. of the High-ß Workshop, Los Alamos (1975), ERDA-76/108

29 Dobrott D.R., Miller R.L.: Flux surface shape and current profile optimization in tokamak. Gen. El. Rep. GA-A 140 10 (1976)

30 Borraß, K.: The influence of the radial density and temperature profiles on the mean fusion power density in a tokamak. IPP Internal Report Syst. Stud. No. 7 (1976)

31 Stringer T.E.: Radial profile of α-particle heating in a tokamak. Plasma Phys. 16, 651 (1974)

32 Pfirsch D., Düchs D.: Distribution of α-particles in large tokamak and reactor plasmas. 7th Europ. Fus. Conf., Lausanne, 24 (1975)

33 Gibson A.: Parameter requirements for the plasma in a toroidal reactor. EUR 4999e, ERICE (1972), p. 15

34 Dean S.O. et al.: Status and objective of tokamak systems for fusion research. Rep.: WASH-1295 UC-20 (1974)